High phenotypic plasticity at the dawn of the eosauropterygian radiation (#82319)

First submission

Guidance from your Editor

Please submit by **15 May 2023** for the benefit of the authors (and your token reward) .

Structure and Criteria
Please read the 'Structure and Criteria' page for general guidance.

Raw data check
Review the raw data.

Image check
Check that figures and images have not been inappropriately manipulated.

If this article is published your review will be made public. You can choose whether to sign your review. If uploading a PDF please remove any identifiable information (if you want to remain anonymous).

Files

Download and review all files from the materials page.

3 Figure file(s)
3 Table file(s)
2 Raw data file(s)
1 Other file(s)

Structure and Criteria

Structure your review

The review form is divided into 5 sections. Please consider these when composing your review:

1. **BASIC REPORTING**
2. **EXPERIMENTAL DESIGN**
3. **VALIDITY OF THE FINDINGS**
4. General comments
5. Confidential notes to the editor

🗋 You can also annotate this PDF and upload it as part of your review

When ready submit online.

Editorial Criteria

Use these criteria points to structure your review. The full detailed editorial criteria is on your guidance page.

BASIC REPORTING

- Clear, unambiguous, professional English language used throughout.
- Intro & background to show context. Literature well referenced & relevant.
- Structure conforms to PeerJ standards, discipline norm, or improved for clarity.
- Figures are relevant, high quality, well labelled & described.
- Raw data supplied (see PeerJ policy).

EXPERIMENTAL DESIGN

- Original primary research within Scope of the journal.
- Research question well defined, relevant & meaningful. It is stated how the research fills an identified knowledge gap.
- Rigorous investigation performed to a high technical & ethical standard.
- Methods described with sufficient detail & information to replicate.

VALIDITY OF THE FINDINGS

- *i* Impact and novelty not assessed. *Meaningful* replication encouraged where rationale & benefit to literature is clearly stated.
- All underlying data have been provided; they are robust, statistically sound, & controlled.
- Conclusions are well stated, linked to original research question & limited to supporting results.

Standout reviewing tips

The best reviewers use these techniques

Tip	*Example*
Support criticisms with evidence from the text or from other sources	*Smith et al (J of Methodology, 2005, V3, pp 123) have shown that the analysis you use in Lines 241-250 is not the most appropriate for this situation. Please explain why you used this method.*
Give specific suggestions on how to improve the manuscript	*Your introduction needs more detail. I suggest that you improve the description at lines 57- 86 to provide more justification for your study (specifically, you should expand upon the knowledge gap being filled).*
Comment on language and grammar issues	*The English language should be improved to ensure that an international audience can clearly understand your text. Some examples where the language could be improved include lines 23, 77, 121, 128 – the current phrasing makes comprehension difficult. I suggest you have a colleague who is proficient in English and familiar with the subject matter review your manuscript, or contact a professional editing service.*
Organize by importance of the issues, and number your points	*1. Your most important issue* *2. The next most important item* *3. ...* *4. The least important points*
Please provide constructive criticism, and avoid personal opinions	*I thank you for providing the raw data, however your supplemental files need more descriptive metadata identifiers to be useful to future readers. Although your results are compelling, the data analysis should be improved in the following ways: AA, BB, CC*
Comment on strengths (as well as weaknesses) of the manuscript	*I commend the authors for their extensive data set, compiled over many years of detailed fieldwork. In addition, the manuscript is clearly written in professional, unambiguous language. If there is a weakness, it is in the statistical analysis (as I have noted above) which should be improved upon before Acceptance.*

High phenotypic plasticity at the dawn of the eosauropterygian radiation

Antoine Laboury [Corresp., 1] , Torsten M Scheyer [2] , Nicole Klein [3] , Tom Stubbs [4] , Valentin Fischer [1]

[1] Evolution & Diversity Dynamics Lab, Université de Liège, Liège, Belgium

[2] Department of Palaeontology, University of Zurich, Zurich, Switzerland

[3] Institute of Geosciences, Paleontology, University of Bonn, Bonn, Germany

[4] School of Earth Sciences, University of Bristol, Bristol, United Kingdom

Corresponding Author: Antoine Laboury
Email address: a.laboury@uliege.be

The Triassic biotic recovery following the Permian–Triassic boundary mass extinction is marked by a rapid radiation of reptiles secondarily adapted to marine environments. The initial radiation of Eosauropterygia, the most speciose clade, is a key part of that rise to dominance of marine reptiles. Recent studies on Mesozoic marine reptile disparity highlighted that eosauropterygians had greatest morphological diversity during the Middle Triassic, with the co-occurrence of Pachypleurosauroidea, Nothosauroidea and Pistosauroidea, mostly along the margins of the Tethys Ocean. However, these previous studies quantitatively analysed the disparity of Eosauropterygia as a whole without focussing on Triassic taxa. As a result, our understanding of the diversification of Middle Triassic eosauropterygians along the Tethys and the pattern of their morphospace occupation is highly limited. Our multivariate morphometric analyses highlight clear ecomorphological distinction between the three clades, with no evidence of important whole-body convergent evolution. This pattern is mostly due to craniodental differences and strongly linked to feeding specializations. We also highlight a clear regional disparity pattern evolution differing between nothosauroids and pachypleurosauroids of which the latter likely experienced a remarkable diversification in the eastern Tethys during the Pelsonian. Our results demonstrate that the high phenotypic plasticity characterizing the evolution of the pelagic plesiosaurians was already present in their Triassic ancestors, and represents a plesiomorphic condition for the entire Eosauropterygia.

1

High phenotypic plasticity at the dawn of the eosauropterygian radiation

4

5 Antoine Laboury[1], Torsten M. Scheyer[2], Nicole Klein[3], Thomas L. Stubbs[4], Valentin Fischer[1]

6 [1] Evolution & Diversity Dynamics Lab, University of Liège, Liège, Belgium

7 [2] Department of Palaeontology, University of Zurich, Zurich, Switzerland

8 [3] University of Bonn, Institute of Geosciences, Paleontology, Bonn, Germany

9 [4] School of Earth Sciences, University of Bristol, Bristol, United Kingdom

10

11 Corresponding author:

12 Antoine Laboury[1]

13 Email address: a.laboury@uliege.be

14

15 **Abstract**

16 The Triassic biotic recovery following the Permian–Triassic boundary mass extinction is marked

17 by a rapid radiation of reptiles secondarily adapted to marine environments. The initial radiation

18 of Eosauropterygia, the most speciose clade, is a key part of that rise to dominance of marine

19 reptiles. Recent studies on Mesozoic marine reptile disparity highlighted that eosauropterygians

20 had greatest morphological diversity during the Middle Triassic, with the co-occurrence of

21 Pachypleurosauroidea, Nothosauroidea and Pistosauroidea, mostly along the margins of the

22 Tethys Ocean. However, these previous studies quantitatively analysed the disparity of

23 Eosauropterygia as a whole without focussing on Triassic taxa. As a result, our understanding of

24 the diversification of Middle Triassic eosauropterygians along the Tethys and the pattern of their

25 morphospace occupation is highly limited. Our multivariate morphometric analyses highlight

26 clear ecomorphological distinction between the three clades, with no evidence of important

27 whole-body convergent evolution. This pattern is mostly due to craniodental differences and

28 strongly linked to feeding specializations. We also highlight a clear regional disparity pattern

29 evolution differing between nothosauroids and pachypleurosauroids of which the latter likely

30 experienced a remarkable diversification in the eastern Tethys during the Pelsonian. Our results

31 demonstrate that the high phenotypic plasticity characterizing the evolution of the pelagic

32 plesiosaurians was already present in their Triassic ancestors, and represents a plesiomorphic

33 condition for the entire Eosauropterygia.

34

Introduction

The Triassic biotic recovery following the Permian–Triassic boundary mass extinction (PTME) represents a crucial episode in Earth's history, characterized by the colonization of the oceans by reptiles and the emergence of modern trophic networks in these aquatic ecosystems that are still in place today (Benton et al., 2013; Fröbisch et al., 2013; Scheyer et al., 2014; Liu et al., 2014; Kelley & Pyenson, 2015; Foffa et al., 2018; Vermeij & Motani, 2018; Huang et al., 2020; Sander et al., 2021; Dai et al., 2023). These marine reptiles dominated the whole Mesozoic and explored numerous ecological niches as demonstrated by their great ecomorphological diversification (Bardet et al., 2014; Stubbs & Benton, 2016; Foffa et al., 2018; Moon & Stubbs, 2020; Reeves et al., 2021; Sander et al., 2021; MacLaren et al., 2022; Fischer et al., 2022). Marine reptiles experienced an unprecedented burst of diversification during the Middle Triassic, likely driven by the novel ecological opportunities provided by the shallow epicontinental seas connected to the Paleotethys and Panthalassa oceans (Benson & Butler, 2011; Stubbs & Benton, 2016; Moon & Stubbs, 2020; Reeves et al., 2021). Sauropterygia is the most speciose and the longest-living (Olenekian – Maastrichtian; e.g. Benson et al., 2010; Jiang et al., 2014) clade of marine reptiles and its members were key components of marine trophic chains for the entire Mesozoic. This clade is divided into two major lineages, the durophagous Placodontia and the disparate Eosauropterygia which includes the lizard-like pachypleurosauroids, the flat headed nothosauroids, and the long-necked pistosauroids, in which plesiosaurians are nested (Rieppel, 2000; Motani, 2009). The Triassic representatives of Sauropterygia are essentially restricted to the western and eastern margins of the Paleotethys (outcropping in present-day Europe and China, respectively) (Rieppel, 2000; Bardet et al., 2014) even if some taxa such as *Corosaurus* and *Augustasaurus* and remains with nothosauroidean affinity have been found in Eastern

58   ~~nthalassea~~ as well (outcropping in present-day North America) (Case, 1936; Sander, Rieppel

59   & Bucher, 1997; Rieppel, 2000; Bardet et al., 2014; Scheyer, Neuman & Brinkman, 2019).

60   Recent studies of marine reptile disparity through the entire Mesozoic have demonstrated

61   that sauropterygians became the most disparate clade by the Anisian (Stubbs & Benton, 2016;

62   Reeves et al., 2021) and that morphological diversity was mostly driven by the emergence of the

63   unique durophagous adaptations of placodonts (Stubbs & Benton, 2016; Reeves et al., 2021;

64   Fischer et al., 2022). Concerning eosauropterygians, qualitative observations in the fossil record

65   reveal a diversification of morphologies related to both their feeding strategies (Rieppel, 2002)

66   and swimming modes during the Middle Triassic (Krahl, Klein & Sander, 2013; Klein et al.,

67   2016; Xu et al., 2022). Quantitative analyses suggest a burst in skull size and high disparity

68   during that period (Stubbs & Benton, 2016), associated with the appearance of small-sized

69   pachypleurosauroids and gigantic nothosaurians (Liu et al., 2014). Post-Triassic sauropterygians

70   (i.e. Plesiosauria) would seemingly never again reach such a high disparity even if their

71   evolution was punctuated by periods of high morphological diversification, craniodental

72   convergences and variations in neck elongation (Stubbs & Benton, 2016; Fischer et al., 2018,

73   2020; Reeves et al., 2021).

74   However, studies which have analyzed the disparity of Sauropterygia mostly consider the

75   clade as a whole, or only investigate the morphological evolution of the derived plesiosaurians,

76   leaving thus the Triassic clades relatively understudied. As a consequence, little is known about

77   the diversification dynamics and morphospace occupation of the Triassic eosauropterygian

78   clades, as well as the existence of phenotypical convergence amongst them. Recent analyses of

79   the temporal trends of vertebrate diversity have highlighted the importance of analyzing regional

80   dynamics, as the structure of the fossil record (i.e. which niches are sampled and how) fluctuates

81 geographically (Close et al., 2020; MacLaren et al., 2022). Qualitative evidence suggests that

82 Middle Triassic eosauropterygians display geographical differences in their assemblages:

83 pachypleurosauroids found in the Anisian of China (Luoping and Panxian biota) appear to have

84 greater morphological diversity, especially in the craniodental region (Wu et al., 2011; Cheng et

85 al., 2012, 2016; Xu et al., 2022, 2023) while some European nothosauroids seemed to have

86 developed unique feeding strategies (Rieppel, 1994; de Miguel Chaves, Ortega & Pérez-García,

87 2018).

88 In this paper, we therefore investigate the cranial and postcranial morphological

89 diversification of Middle Triassic eosauropterygians and explore their patterns of morphospace

90 occupation and possible evolutionary convergence. We also characterize the spatiotemporal

91 distribution of their disparity along the Tethys Ocean.

92

93 **Material and methods**

94 **Data**. We gathered a set of thirty-five cranial and postcranial linear measurements on thirty-six

95 Triassic eosauropterygian species (seventeen pachypleurosauroids, sixteen nothosauroids and

96 three pistosauroids; see Table1). We collected data directly from specimens (by a digital calliper

97 with a precision of 0.01 mm), on high-precisions 3D models using Meshlab v2022.02 (Cignoni

98 et al., 2008), or using ImageJ (v.1.53) on first-hand pictures and pictures from the literature,

99 when no other alternative was found. The 3D models were generated with a Creaform

100 HandySCAN 300 laser scanner at resolution varying from 0.2 to 0.5 mm, depending on the size

101 of the specimen and with an Artec Eva white light scanner at resolution ≈0.5 mm. These 3D

102 models are available on MorphoSource:

103 https://www.morphosource.org/projects/000508432/temporary_link/C8LoptLfUfWasUbssNkHo

104   miH?locale=en. These measurements were used to calculate twenty-seven-dimension

105   quantitative morphofunctional ratios with clear biomechanical and architectural implications

106   (Anderson et al., 2011; Stubbs & Benton, 2016; MacLaren et al., 2017, 2022; Fischer et al.,

107   2020; Bennion et al., 2022). In addition to these ratios, we also added the absolute height of the

108   dental crown, as it represents an informative ecological signal in marine predators (Fischer et al.,

109   2022). Finally, we used four discrete traits adapted from Stubbs & Benton (2016) to better

110   characterize the morphology of the teeth and the mandible. Twenty-one traits are devoted to

111   craniodental anatomy and ten sample the postcranial region (Table 2 and see Supplementary

112   Information for a definition of each trait). All species have been submitted to a 40%

113   completeness threshold to prevent any distortions in our ordination analyses caused by an

114   excessive amount of missing data. The initial total amount of missing entries in our dataset

115   before applying the threshold equals 21.01%, with respectively 14.81% and 36.11% for the

116   craniodental and postcranial regions.

117   **Phylogenetic analyses**

118   We generated phylogenetic trees by reanalysing the recently published dataset of Xu et al. (2022)

119   within an implied-weighting maximum parsimony framework, in TNT (v1.5) (Goloboff &

120   Catalano, 2016). We set the maximum number of trees to 100 000 and we used the New

121   Technology Search (ratchet activated: 200 iterations; drift activated: 10 cycles; 10 hits and 10

122   trees per replication). Our phylogenetic analyses were conducted when the concavity constant K

123   was set to 12 and we applied a tree bisection-reconnection (TBR) algorithm on trees recovered

124   by the ratchet to fully explore islands of most parsimonious trees. Our most parsimonious tree

125   has a length of 25.520 and can be visualized in the Supplementary Information (Fig. S1). As the

126   phylogenetic dataset of Xu et al. (2022) does not include all the species we sampled in our

127 ecomorphological dataset, we added manually six species using the literature and the phytools

128 (v0.7-80) and paleotree (v3.3.25) packages (Bapst, 2012; Revell, 2012): we split the OTU

129 *"Neusticosaurus"* of the dataset of Xu et al. (2022) into its three species, *Neusticosaurus pusillus*

130 as the sister taxa of the clade composed of *Neusticosaurus edwardsii* and *Neusticosaurus peyeri*

131 (Klein et al., 2022); *Prosantosaurus scheffoldi* as the sister lineage of the clade comprising

132 *Serpianosaurus* and *Neusticosaurus* (Klein et al., 2022); *Brevicaudosaurus jiyangshanensis* as

133 the sister lineage of Nothosauridae (Shang, Wu & Li, 2020); *Nothosaurus luopingensis* as the

134 sister lineage of *Nothosaurus yangjuanensis* (Shang, Li & Wang, 2022), and *Luopingosaurus*

135 *imparilis* as the sister lineage of *Honghesaurus longicaudalis* (Xu et al., 2023). We pruned the

136 resulting tree by removing all the taxa which have not been included in our ecomorphological

137 dataset, using the ape v5.2 package (Paradis, Claude & Strimmer, 2004). We then time-scaled it

138 using the minimum branch length algorithm, using a minimal value of 0.5 Myr, using the

139 paleotree package (v3.3.25) (Bapst, 2012) (see Supplementary Information Fig. S2). The age

140 range of each species of our dataset is provided in Table1.

141 **Ordination methods, macroevolutionary landscape, and disparity**

142 All analyses were performed in the R statistical environment (v. 4.2.1) (R Core Team, 2021) and

143 followed the protocol established by Fischer et al. (2020) which is designed to visualize the

144 density of trait space occupancy and test for the existence of a macroevolutionary landscape.

145 Each continuous trait in the morphological dataset were z-transformed (assigning to all

146 continuous traits a mean of 0 and a variance of 1) prior to computation of a Gower distance

147 matrix. We chose a Gower distance metric as our dataset contains both continuous and discrete

148 traits. We submitted our distance matrix to a cluster dendrogram analysis using the Ward

149 clustering criterion to visualize the morphological similarities among Triassic eosauropterygians.

150 To evaluate the statistical support of our clustering results, we applied a multiscaled

151 bootstrapping procedure, the 'Approximatively Unbiased P-value' method implemented in the

152 pvclust package (v2.2-0) (Suzuki, Terada & Shimodaira, 2019). This method creates subsamples

153 of different sizes from our original distance matrix. We ran it from 0.5 to 10 times the size of our

154 distance matrix, at increments of 0.5 and 1000 bootstraps per increment. We also created

155 tanglegrams (Fig. S4) using the dendextend package (v.1.16.0) (Galili, 2015) to compare the

156 phylogenetic position and the phenotypic distance of taxa and we tested their correlation by

157 computing Mantell tests (1000 permutations) using the vegan package (v2.5-2) (Oksanen et al.,

158 2019). We ran multivariate morphospace analyses via both principal coordinate analysis (PCoA)

159 applying the Caillez correction for negative eigenvalues, using the ape package (v5.2) (Paradis,

160 Claude & Strimmer, 2004) and non-metric multidimensional scaling (NMDS, dimension=2),

161 using the vegan package (v2.5-2) (Oksanen et al., 2019). We computed phylomorphospaces to

162 visualize the ecomorphological trajectories across the evolution of Triassic eosauropterygians.

163 Density of morphospace occupation was computed using a Kernel two-dimensional density

164 estimate on the NMDS phylomorphospace, using the modified ggphylomorphospace function

165 provided in Fischer et al. (2020). We also computed NMDS ecomorphospaces for the following

166 time bins of Middle Triassic: Bithynian, Pelsonian, Illyrian (substages of the Anisian) and

167 Fassanian and Longobardian (substages of the Ladinian) for the Western and Eastern Tethys

168 provinces. The distribution of skull lengths and width (the maximum distance between left and

169 right quadrates) are reported in Figs. 2C and 2D, respectively.

170 **Convergence analyses**

171 We tested the significance of interclade ecomorphological convergence by applying the C1, C2,

172 C3, and C4 metrics of Stayton (Stayton, 2015) on selected pairs of taxa based on the results of

173   our ordination analyses. The first two metrics quantify the phenotypic distance of a pair of taxa

174   by comparison to the dissimilarity of their respective ancestral nodes while the metric C3 and C4

175   include the total amount of evolution (sum of all phenotypic distances) in the clade defined by

176   the last common ancestor of this pair of taxa. We decided to test possible ecomorphological

177   convergence between the pistosauroid *Wangosaurus brevirostris* and two nothosauroids which

178   are the closest taxa to this taxon in the cluster dendrogram, *Lariosaurus calcagnii* and

179   *Brevicaudosaurus jiyangshanensis.* Even if *Wangosaurus* is phylogenetically found to be the

180   al most pistosauroid in many phylogenetic analyses (Ma et al., 2015; Jiang et al., 2019; Lin et

181   al., 2021; Xu et al., 2022, 2023), its craniodental architecture and limbs seem quite similar to that

182   of nothosauroids (Ma et al., 2015). In our cluster dendrogram (Fig. 2B), the singular

183   nothosauroid *Simosaurus gaillardoti* is found to be morphologically closer to

184   pachypleurosauroids. Therefore, we also decided to investigate the existence of any convergence

185   of *Simosaurus* with the closest pachypleurosauroid in our morphospace, *Qianxisaurus*

186   *chajiangensis* which also possess a peculiar tooth morphology potentially reflecting a hard-shell

187   prey preference (Cheng et al., 2012; Benton et al., 2013; Stubbs & Benton, 2016). We selected

188   our most parsimonious tree (Fig. S2), and we tested the significance of these supposed

189   convergences by evaluating the character evolution under 1000 Brownian simulations using

190   respectively the first two and all axes of the PCoA, generated with the whole-body data and with

191   the only craniodental anatomy for the test including *Simosaurus* as less than 40% of postcranial

192   information is available for this taxon. These analyses have been generated using the convevol

193   package (V1.3) (Stayton, 2018).

194   **Morphofunctional disparity analyses**

195 We used all axes of PCoA to compute a bootstrapped distribution of the total morphofunctional

196 disparity (sum of ranges, 1000 Bootstrap iterations) using the dispRity package (v1.2.3)

197 (Guillerme, 2018), for both Pachypleurosauroidea and Nothosauroidea in the Western and

198 Eastern Tethys regions. The significance of difference between the regional disparities for both

199 clades have been calculated with the non-parametric Wilcoxon test. We also calculated the

200 overall morphofunctional disparity for both clades (Pachypleurosauroidea and Nothosauroidea)

201 independently of the location of the taxa (Fig. S17) and for both regions (western and eastern

202 Tethys) without distinguishing the clades (Fig. S18). Given the small number of pistosauroids in

203 our dataset, we decided to not include them in per-clade analyses, but they are sampled for

204 regional disparities (Fig. S18). Finally, we computed the temporal evolution of the global

205 disparity during the Middle Triassic as a sum of ranges (see Supplementary Information Fig.

206 S20)

207

208 **Results**

209 **Cluster dendrogram, morphospace occupation and evolutionary convergence**

210 A clear division in the cluster dendrogram separates species of the dataset into two extremely

211 robust groups (Fig. 2B). The first one comprises all pistosauroids and all nothosauroids (except

212 for *Simosaurus gaillardoti*). In this one, the primitive pistosauroid *Wangosaurus brevirostris*

213 clusters with two nothosauroids, *Brevicaudosaurus jiyanshanensis* and *Lariosaurus calcagnii*.

214 The second main group in the cluster dendrogram includes all pachypleurosauroids which form a

215 well-defined cluster and *S. gaillardoti*, occupying the most basal position. In the

216 ecomorphospace, the Triassic eosauropterygians tend to globally occupy distinct regions, with

217 the pistosauroids located closer to nothosauroids than to pachypleurosauroids, thus reflecting

218   broad-scale phylogenetic relationships (Fig. 2A). The separation in the morphospace is mainly

219   due to craniodental morphology; the postcranial skeleton appears less plastic and is marked by a

220   large overlap between pachypleurosauroids and nothosauroids (Fig. S14-16).

221   The density of phenotypes shows two main peaks (Fig. 2A). The broader peak occupying

222   negative values along NMDS axis 2 represents the pachypleurosauroidean morphospace while

223   the narrower and more densely populated peak is mainly occupied by nothosauroids, even if *W.*

224   *brevirostris* is located on the periphery. These two peaks are very well separated by a trough

225   with no 'intermediate' species sampled in our dataset excepted *Dawazisaurus brevis*.

226   Pachypleurosauroids tend to occupy a wider portion of the morphospace than

227   nothosauroids located in the right peak of density (without *S. gaillardoti*), reflecting a higher

228   degree of morphological variation (see also Fig. S17B). However, the inclusion of the peculiar

229   *Simosauru*s greatly increases the disparity of nothosauroids (Fig. S17), as it occupies a unique

230   region of the ecomorphospace. Indeed, *S. gaillardoti* is characterized by a brevirostrine skull

231   with no rostral constriction, the presence of homodont durophagous dentition, and a relatively

232   small upper temporal fenestra (Fig. 1K) (Rieppel, 1994), contrasting with the usually gracile,

233   skulls of nothosaurians characterized by extremely elongated temporal region and specialized

234   heterodont piercing dentition (Fig. 1J) (Rieppel, 2002).

235   As previously mentioned, the position of *Wangosaurus* in the morphospace suggests a

236   greater phenotypic resemblance with nothosauroids than with pistosauroids. Our statistical tests

237   of convergence using Stayton's metrics indeed recover *Wangosaurus* as convergent with the

238   nothosauroids present in the same subgroup of the cluster dendrogram (i.e. *Brevicaudosaurus*

239   *jiyangshanensis* and *Lariosaurus calcagnii*) for every metric, no matter the number of PCoA

240   axes used (Table 3). However, the significance of this evolutionary convergence could be

241 debated due to persisting uncertainties concerning the phylogenetic affinities of *Wangosaurus*.

242 This taxon is often recovered as the basalmost pistosauroid (Ma et al., 2015; Jiang et al., 2019;

243 Lin et al., 2021; Xu et al., 2022, 2023, as well as our study) but some studies recovered it as a

244 basal nothosauroidean instead (Shang, Wu & Li, 2020; Wang et al., 2022). For this reason, we

245 also tested the morphological convergence of *Wangosaurus* with *B. jiyangshanensis* and *L.*

246 *calcagnii* by forcing *Wangosaurus* as a nothosauroidean (see Matériel and Methods, section

247 phylogenetic analyses). *Wangosaurus* is still found to be statistically convergent with *B.*

248 *jiyangshanensis* when considering the first two axes of the PCoA (Table 3) but the convergence

249 with *L. calcagnii* is this time less supported or entirely absent when using respectively the first

250 two or all axes of the PCoA (Table 3). Evidence of craniodental convergence between

251 *Simosaurus* and *Qianxisaurus chajiangensis* is not statistically significant (Table 3) when using

252 the first two axis of the PCoA and completely absent when all axes of the PCoA are used.

253

254 **Regional and temporal patterns of disparity**

255 Pachypleurosauroids and nothosauroids each evolved an approximate equal amount of disparity,

256 even if nothosauroids appears to be slightly more disparate (p-value < 0.00001) (Fig. S17A).

257 This difference in magnitude is mainly due to the unique craniodental morphology of *S.*

258 *gaillardoti*. By removing this taxon and comparing the two peaks of density occupation in the

259 morphospaces (Fig. 2A) pachypleurosauroids appear much more diverse ecomorphologically (p-

260 value < 0.00001) (Fig. S17B). The western Tethyan faunal province records a greater amount of

261 disparity than the eastern Tethyan one (p-value < 0.00001) (Fig. S18A), but this difference is

262 once again exaggerated by the presence of *Simosaurus* (p-value < 0.00001) (Fig. S18B). Our

263 results also show a strong geographical differentiation in the amount of ecomorphological

264   disparity of the two clades. Pachypleurosauroids are clearly more disparate in the eastern

265   Tethyan realm (p-value=0) (Fig. 3A) whereas nothosauroids have a disparity maximum in the

266   western Tethyan realm (p-value=0) (Fig. 3B) even with the absence of *Simosaurus* (p-value=0)

267   (Fig. S19). These regional patterns can be visualized in the morphospace occupation of each

268   geographical regions (Fig. 3D and J). Furthermore, the temporal evolution of disparity seems to

269   also vary within these two regions (Fig. 3D-L). In the eastern Tethyan realm, the disparity

270   maximum is recorded during the Pelsonian, Middle Anisian, with the diversification of

271   pachypleurosauroids (Fig. 3K) while the ecomorphological diversification of eosauropterygians,

272   mostly nothosauroids, occurs during the Fassanian, early Ladinian in the western Tethyan realm

273   (Fig. 3H). All these results therefore tend to highlight a strong geographical and temporal

274   decoupling in the ecomorphological diversification of Triassic eosauropterygians.

275

276   **Discussion**

277   **The early evolutionary trajectories of Triassic eosauropterygians reflect dietary**

278   **specialization**

279   Our ordination analyses provide new quantitative insights on the diversification of Triassic

280   eosauropterygians and reveal a global colonization of distinct ecomorphospaces for each clade

281   (with the exception of *Wangosaurus*). This absence of overlap during their "early burst"

282   radiation (Stubbs & Benton, 2016) reflects the influence of developmental constraints among

283   clades and supports the inference of a substantial and rapid trophic specialization in

284   eosauropterygians, mainly reflected in craniodental architecture and body size (Rieppel, 2002).

285   In a previous study which aimed to investigate the feeding mechanics in Triassic early

286   sauropterygians by reconstructing their jaw adductor musculature, Rieppel (2002) highlighted

287   the near absence of an overlap in the inferred feeding strategies of Triassic eosauropterygians.

288   On one hand, the craniodental architecture of pachypleurosauroids, which are usually small-sized

289   (rarely exceeding cm according Rieppel (2000)) is indeed characterized by a rounded, short

290   and blunt snout, a very short symphysis and a homodont peg-like dentition, strongly suggesting

291   that they have captured their prey by suction feeding, followed by a rapid snapping bite (Rieppel,

292   2002; Xu et al., 2023). Pachypleurosauroids likely evolved a wider array of feeding strategies

293   through time, however. Xu et al. (2023) reported a progressive reduction in the length of the

294   hyoid apparatus and an increase in snout length, involving a gradual shift away from suction

295   feeding for some derived species mostly in eastern Tethys (found at negative NMDS axes 2

296   values on Fig. 2A) (Wu et al., 2011; Cheng et al., 2012; Xu et al., 2023). On the other hand,

297   nothosauroids and pistosauroids likely used their narrow and 'pincer jaw', to conduct sideward-

298   directed snapping bites (Rieppel, 2002). Their skull morphology and dentition suggest, here also,

299   a range of food procurement strategies (Rieppel, 2002). The dentition and the cranial architecture

300   of pistosauroids should be more suitable to puncture prey (Rieppel, 2002), while the presence of

301   procumbent and enlarged fangs in nothosauroids might have served as a fish-trap (Chatterjee &

302   Small, 1989; Rieppel, 2002). Large species such as *L. calcagnii* and *N. giganteus* or *N. zhangi*

303   could have nevertheless occupied the top of the food chain in their ecosystems and preyed on

304   smaller marine reptiles (Tschanz, 1989; Rieppel, 2002; Liu et al., 2014). The isolated position of

305   *S. gaillardoti* with respect to other nothosauroids in the ecomorphospace is mainly explained by

306   its unique feeding strategy as it is the only eosauropterygian to have developed a ~~rophageous~~

307   dentition to crush hard-shelled preys such as ammonoids or hard-scaled fishes (Rieppel, 1994,

308   2002; Klein & Griebeler, 2016; Klein, Eggmaier & Hagdorn, 2022). The magnitude of

309   durophagy in *Simosaurus* is however not comparable to that of placodont sauropterygians which

310   possess a much more robust mandible and teeth highly modified into low labial bulbs and lingual

311   tooth plates (Rieppel, 2002; Neenan, Klein & Scheyer, 2013; Neenan et al., 2015).

312   The postcranial anatomy of Triassic eosauropterygians appears to be less plastic than

313   their craniodental skeleton, which is also possibly the case in short-necked plesiosaurians

314   (besides relative neck length) (O'Keefe, 2002; Fischer et al., 2020). This homogeneity in the

315   morphological diversification of the postcranial region may reflect a conservative locomotion

316   mode in shallow water intraplatform basins, through full body oscillation (Carroll, Gaskill &

317   Whittington, 1985; Rieppel & Lin, 1995; Rieppel, 2000; Neenan et al., 2017; Krahl, 2021; Xu et

318   al., 2022; Klein, Eggmaier & Hagdorn, 2022). However, recent studies suggest the use of

319   forelimbs in propulsion among nothosauroids (Zhang et al., 2014; Klein et al., 2015; Krahl,

320   2021; Klein, Eggmaier & Hagdorn, 2022), thus contrasting with the strict anguilliform

321   swimming seen in pachypleurosauroids (Sander, 1989; Xu et al., 2022; Gutarra & Rahman,

322   2022). It is noteworthy to mention that pistosauroids occupied a portion of the ecomorphospace

323   that has not been colonized by any other eosauropterygians, possibly reflecting the transition

324   from the undulating non-pistosauroids to the pelagic paraxial swimming seen in plesiosaurians

325   (Sato et al., 2014b).

326   Many of the species we analysed coexisted, suggesting that the range of morphologies

327   occupied reflects colonization of multiple niches and, perhaps, niche partitioning. The fairly

328   rapid ecomorphological specialization of eosauropterygians is probably best understood in the

329   context of increasing complexity of marine trophic webs of the shallow marine and coastal

330   environments of the Tethys during the Middle Triassic, following the recovery of the PTME

331   (Benton et al., 2013; Scheyer et al., 2014; Liu et al., 2014, 2021; Li & Liu, 2020; Dai et al.,

332   2023). Indeed, such a diversification pattern is not exclusive of eosauropterygians and have also

333   been detected in ichthyosaurians, tanystropheids, and saurichthyid fishes as well (Rieppel, 1992;

334   Benton et al., 2013; Wu, Sun & Fang, 2017; Spiekman et al., 2020; Bindellini et al., 2021).

335   **Regional diversification patterns in eosauropterygians**

336   Our results quantitatively reveal for the first-time a pervasive regional difference in the disparity

337   of the eosauropterygian assemblages along the Tethys margins suggesting a different

338   biogeographical diversification for pachypleurosauroids and nothosauroids. Pachypleurosauroids

339   seemed to undergo a remarkable ecomorphological radiation during the Pelsonian in the eastern

340   Tethyan realm, rapidly after their earliest appearance in the fossil record of that region (Jiang et

341   al., 2014). This diversification mostly occurred in the Luoping, and also in the Panxian biotas,

342   leading to the coexistence of numerous species with distinct feeding strategies (see the

343   craniodental architecture of *Luopingosaurus* Xu et al. (2023), *Diandongosaurus* Sato et al.

344   (2014a), *Wumengosaurus* Wu et al. (2011)) or unique swimming capabilities among

345   pachypleurosauroids (e.g. *Honghesaurus* Xu et al. (2022)) (Wu et al., 2011; Benton et al., 2013;

346   Sato et al., 2014a; Shang & Li, 2015; Cheng et al., 2016; Liu et al., 2021; Xu et al., 2022, 2023).

347   By comparison, European and more specifically the Alpine pachypleurosauroids are

348   morphologically similar (Rieppel, 2000; Renesto, Binelli & Hagdorn, 2014; Beardmore &

349   Furrer, 2016; Klein et al., 2022) and thus characterized by lower values of disparity. However,

350   the validity of the taxonomic variability of Chinese pachypleurosauroids could be questioned.

351   With the exception of the abundant *Keichousaurus hui* for which the ontogenetic series is well

352   known (Lin & Rieppel, 1998; Cheng et al., 2009), the identification of new species in the

353   eastern Tethys mostly relies on the examination of few fossils, sometime only single specimen

354   without considering ontogenetic and intraspecific variations of preexisting species. Without a

355   thorough taxonomic reinvestigation of the material, the taxonomic diversity of these Chinese

356   pachypleurosauroids could therefore be overestimated which could also affect our regional

357   disparity patterns.

358   The nothosauroids have been found to be more abundant and disparate in the western

359   Tethys in comparison to their Chinese relatives which have less disparity in our analyses (Fig.

360   3C). The total ecomorphological disparity of European nothosauroids is potentially

361   underestimated in our analyses by the absence of the peculiar but fragmentary simosaurid

362   *Paludidraco multidentatus* from the Upper Triassic of Spain (de Miguel Chaves, Ortega &

363   Pérez-García, 2018), whose unique anatomy suggest a manatee-like feeding and locomotion

364   mode (de Miguel Chaves, Ortega & Pérez-García, 2018). The unique morphologies of

365   *Paludidraco* and *Simosaurus* would attest to the higher potential of diversification in feeding

366   strategies in primitive European nothosauroids, compared to the more derived nothosaurians

367   which appeared more similar, excepted in their size (Rieppel & Wild, 1996; Liu et al., 2014).

368   Variation in the quality of the fossil record, notably Lagerstätten effects can be a

369   powerful driver of spatiotemporal differences in diversity and can have complex impacts on

370   disparity trends (Benson et al., 2010; Benson & Butler, 2011; Sutherland et al., 2019). In our

371   study, both the eastern and western Tethys localities have been intensively sampled overtime,

372   especially in Luoping, Panxian, Xingyi (China), and Monte San Giorgio and Winterswijk

373   (Europe), allowing comparisons between these two regions (Rieppel, 2000; Furrer, 2003; Motani

374   et al., 2008; Benton et al., 2013; Renesto, Binelli & Hagdorn, 2014; Heijne, Klein & Sander,

375   2019; Xu et al., 2022). Nevertheless, the Chinese assemblages which have been characterized as

376   exceptional in terms of faunal communities represent temporally disconnected 'snapshots' of the

377   Pelsonian (Luoping and Panxian) and Longobardian (Xingyi) while European localities have

378   produced a rather continuous Middle Triassic time series (Rieppel, 2000; Röhl et al., 2001;

379   Furrer, 2003; Hu et al., 2011; Benton et al., 2013).

380   Thus, if not spatial heterogeneities of the fossil record, what drives the observed

381   differences among eosauropterygian phenotypes between Tethysian provinces? Both regions

382   were likely subtropical shallow platform environments characterized by a rather similar

383   vertebrate assemblages mainly composed of saurichthyid fishes (Wu et al., 2009; Benton et al.,

384   2013; Maxwell et al., 2015, 2016), mixosaurid ichthyosaurians (Brinkmann, 1998; Motani, 1999;

385   Maisch, Matzke & Brinkmann, 2006; Jiang et al., 2006, 2007; Benton et al., 2013; Liu et al.,

386   2013), placodonts (Neenan, Klein & Scheyer, 2013; Neenan et al., 2015), thalattosaurians

387   (Cheng, 2003; Müller, 2005; Cheng et al., 2010), and tanystropheids (Rieppel, Li & Fraser,

388   2008; Spiekman et al., 2020), in addition to eosauropterygians. This broad-brush homogeneity in

389   the faunae is expected to result from a dispersal route along coastlines of the Tethys, allowing

390   exchanges between the European and Chinese provinces (Rieppel, 1999; Bardet et al., 2014).

391   Drivers of this decoupling in disparity among pachypleurosauroids and nothosauroids

392   remains unclear and require a thorough reinvestigation of the differences between ecosystems

393   along the Tethys Ocean. However, this variation reveals the importance of analysing regional

394   dynamics rather than a summed-up, oversimplified signal when spatial heterogeneities appeared

395   strong, as recently demonstrated by Close et al. (2020) and MacLaren et al. (2022).

396   **Eosauropterygia, a plastic clade throughout most of its history**

397   Eosauropterygia and Ichthyosauria were the longest-lived clades of Mesozoic marine reptiles.

398   The shape of their radiation and subsequent diversification has been analysed in terms of skull

399   size, mandible shape, and skeletal characters suggesting an early-burst radiation, that produced a

400   high variety of morphologies in the shallow marine environments during the Middle Triassic

401 (Stubbs & Benton, 2016; Moon & Stubbs, 2020). However, the remodelling of marine

402 ecosystems caused by regression events during the Late Triassic profoundly altered their

403 evolutionary history and only pelagic morphotypes have thought to survive across the Triassic –

404 Jurassic boundary (McGowan, 1997; Benson et al., 2010; Benson & Butler, 2011; Thorne, Ruta

405 & Benton, 2011; Dick & Maxwell, 2015; Wintrich et al., 2017). This marine faunistic turnover is

406 thus associated with a quantitative drop in the disparity coupled with the emergence of

407 parvipelvians and plesiosaurians in the Early Jurassic (Dick & Maxwell, 2015; Stubbs & Benton,

408 2016; Moon & Stubbs, 2020). While the disparity of ichthyosaurians still constantly decreased

409 through the rest of the Mesozoic (Thorne, Ruta & Benton, 2011; Dick & Maxwell, 2015; Fischer

410 et al., 2016), post-Early Jurassic plesiosaurians has been characterized by an impressive

411 ecomorphological diversity (O'Keefe, 2002; Benson & Druckenmiller, 2014; Fischer et al.,

412 2020). Indeed, the evolutionary history of plesiosaurians has been marked by the recurrence of

413 superficially similar phenotypes in weakly related lineages (e.g. 'plesiosauromorph' vs

414 'pliosauromorph' or 'longirostrine' vs 'latirostrine' in short-necked derived plesiosaurians) over

415 time (O'Keefe, 2002; Fischer et al., 2017, 2018, 2020) and by the ability to innovate in their

416 feeding strategies (O'Keefe et al., 2017).

417   This great ecomorphological diversification demonstrates that plesiosaurians were

418 capable of producing a large variety of forms and were therefore characterized by a high

419 phenotypic plasticity which may have helped them to withstand or adapt to changes in the

420 ecosystems over the Jurassic and the Cretaceous. The remarkable feeding specialization among

421 Middle Triassic eosauropterygians coupled with their ability to experience distinct regional

422 pattern of diversification also highlight such a phenotypic plasticity in addition to their high

423 developmental plasticity identified by the diversity of their life history traits (Klein & Griebeler,

PeerJ

424   2018; Griebeler & Klein, 2019). Our results would thus suggest that eosauropterygians have

425   always displayed a wide range of variation in their craniodental architecture and that a constant

426   morphological plasticity have characterized their overall evolutionary history; the initial

427   plesiosaurian radiation during the Early Jurassic being the exception with the lowest values of

428   disparity recorded (Benson, Evans & Druckenmiller, 2012; Benson & Druckenmiller, 2014;

429   Stubbs & Benton, 2016).

430

431   **Conclusions**

432   In the evolutionary history of Eosauropterygia, the Middle Triassic represents a crucial period

433   marked by their initial and expanding diversification, recording their maximum of disparity. This

434   diversification led to a clear craniodental distinction and feeding specialization among

435   pachypleurosauroids, nothosauroids and pistosauroids, suggesting low interspecific competition

436   in the shallow intraplatform basins bordering the Tethys Ocean. These clades occupy well

437   distinct regions of the ecomorphospace and the nothosauroidean *Simosaurus* is very isolated

438   from the rest of the clade due to unique durophageous adaptations among Eosauropterygia. On

439   the other hand, the postcranial anatomy of the Triassic eosauropterygians shows less

440   diversification and is largely similar between pachypleurosauroids and nothosauroids while the

441   pistosauroids appears slightly distinct. This morphological homogeneity suggests a decoupling in

442   the evolution of the craniodental and the postcranial morphologies, similarly to what has been

443   proposed for derived, short-necked plesiosaurians.

444   Our analyses also demonstrate that the disparity of pachypleurosauroids and

445   nothosauroids differs along the Tethys margins, reflecting regional variations in their disparity.

446   The eastern Tethys during the Pelsonian, Middle Anisian, represented a unique 'hotspot' for the

447 morphological diversification of pachypleurosauroids in which various craniodentally distinct

448 taxa co-occurred. The western margin of the Tethys was dominated by nothosauroids, and their

449 disparity has been mainly increased by the morphology of *Simosaurus*. This regional variation in

450 disparity would suggests that Triassic eosauropterygians diversified in a different way depending

451 on the biotic and abiotic features of the ecosystems. This high phenotypic plasticity also

452 characterizes the evolution of post-Triassic plesiosaurians which have undergone remarkable

453 morphological diversification events during their evolutionary history, suggesting that it would

454 represent an ancestral trait of Eosauropterygia.

455

465

466 **References**

467 Anderson PSL, Friedman M, Brazeau MD, Rayfield EJ. 2011. Initial radiation of jaws

468   demonstrated stability despite faunal and environmental change. *Nature* 476:206–209. DOI:

469   10.1038/nature10207.

470

471   Bapst DW. 2012. paleotree: an R package for paleontological and phylogenetic analyses of

472   evolution. *Methods in Ecology and Evolution* 3:803–807. DOI: 10.1111/j.2041-

473   210X.2012.00223.x.

474

475   Bardet N, Falconnet J, Fischer V, Houssaye A, Jouve S, Pereda Suberbiola X, Pérez-García A,

476   Rage J-CJ-C, Vincent P. 2014. Mesozoic marine reptile palaeobiogeography in response to

477   drifting plates. *Gondwana Research* 26:869–887. DOI: 10.1016/j.gr.2014.05.005.

478

479   Beardmore S, Furrer H. 2016. Preservation of Pachypleurosauridae (Reptilia; Sauropterygia)

480   from the Middle Triassic of Monte San Giorgio, Switzerland. *Neues Jahrbuch für Geologie*

481   *und Paläontologie - Abhandlungen* 280:221–240. DOI: 10.1127/njgpa/2016/0578.

482

483   Bennion RF, MacLaren JA, Coombs EJ, Marx FG, Lambert O, Fischer V. 2022. Convergence

484   and constraint in the cranial evolution of mosasaurid reptiles and early cetaceans.

485   *Paleobiology*:1–17. DOI: 10.1017/pab.2022.27.

486

487   Benson RBJ, Butler RJ. 2011. Uncovering the diversification history of marine tetrapods:

488   ecology influences the effect of geological sampling biases. In: McGowan AJ, Smith AB

489   eds. *Comparing the geological and fossil records: implications for biodiversity studies*.

490   London: Geological Society, Special Publications, 191–208.

491

492   Benson RBJ, Butler RJ, Lindgren J, Smith AS. 2010. Mesozoic marine tetrapod diversity: mass

493   extinctions and temporal heterogeneity in geological megabiases affecting the vertebrates.

494   *Proceedings of the Royal Society B: Biological Sciences* 277:829–834. DOI:

495   10.1098/rspb.2009.1845.

496

497   Benson RBJ, Druckenmiller PS. 2014. Faunal turnover of marine tetrapods during the Jurassic–

498   Cretaceous transition. *Biological Reviews* 89:1–23. DOI: 10.1111/brv.12038.

499

500   Benson RBJ, Evans M, Druckenmiller PS. 2012. High diversity, low disparity and small body

501   size in plesiosaurs (Reptilia, Sauropterygia) from the Triassic–Jurassic boundary. *PLoS*

502   *ONE* 7:e31838.

503   Benton MJ, Zhang Q, Hu S, Chen Z-Q, Wen W, Liu J, Huang J, Zhou C, Xie T, Tong J, Choo B.

504   2013. Exceptional vertebrate biotas from the Triassic of China, and the expansion of marine

505   ecosystems after the Permo-Triassic mass extinction. *Earth-Science Reviews* 125:199–243.

506   DOI: 10.1016/j.earscirev.2013.05.014.

507

508   Bindellini G, Wolniewicz AS, Miedema F, Scheyer TM, Dal Sasso C. 2021. Cranial anatomy of

509   *Besanosaurus leptorhynchus* Dal Sasso & Pinna, 1996 (Reptilia: Ichthyosauria) from the

510   Middle Triassic Besano Formation of Monte San Giorgio, Italy/Switzerland: taxonomic and

511   palaeobiological implications. *PeerJ* 9:e11179. DOI: 10.7717/peerj.11179.

512

513 Brinkmann W. 1998. Die Ichthyosaurier (Reptilia) aus der Grenzbitumenzone (Mitteltrias) des

514   Monte San Giorgio (Tessin, Schweiz) - neue Ergebnisse. *Vierteljahrsschrift der*

515   *Naturforschenden Gesellschaft in Zürich* 143:165–177.

516

517 Carroll RL, Gaskill P, Whittington HB. 1985. The nothosaur *Pachypleurosaurus* and the origin

518   of plesiosaurs. *Philosophical Transactions of the Royal Society of London. B, Biological*

519   *Sciences* 309:343–393. DOI: 10.1098/rstb.1985.0091.

520

521 Case EC. 1936. A nothosaur from the Triassic of Wyoming. *University of Michigan*

522   *Contributions form the Museum of Paleontology* 5:1–36.

523

524 Chatterjee S, Small BJ. 1989. New plesiosaurs from the Upper Cretaceous of Antarctica.

525   *Geological Society, London, Special Publications* 47:197–215. DOI:

526   10.1144/GSL.SP.1989.047.01.15.

527

528 Cheng L. 2003. A new species of Triassic Thalattosauria from Guanling, Guizhou. *Geological*

529   *Bulletin of China* 22:274–277.

530

531 Cheng L, Chen X-H, Zhang B-M, Wang X-F. 2010. A new material of Thalattosauria (Reptilia:

532   Diapsida) from the middle triassic of Luoping, Yunnan province. *Diqiu Kexue - Zhongguo*

533   *Dizhi Daxue Xuebao/Earth Science - Journal of China University of Geosciences* 35:507–

534   511. DOI: 10.3799/dqkx.2010.065.

535

536 Cheng Y-N, Holmes R, Wu X-C, Alfonso N. 2009. Sexual dimorphism and life history of

537 *Keichousaurus hui* (Reptilia: Sauropterygia). *Journal of Vertebrate Paleontology* 29:401–

538 408. DOI: 10.1671/039.029.0230.

539

540 Cheng Y-N, Wu X-C, Sato T, Shan H-Y. 2012. A new eosauropterygian (Diapsida,

541 Sauropterygia) from the Triassic of China. *Journal of Vertebrate Paleontology* 32:1335–

542 1349. DOI: 10.1080/02724634.2012.695983.

543

544 Cheng Y, Wu X, Tamaki S, Shan, His-yin. 2016. *Dawazisaurus brevis*, A New Eosauropterygian

545 From the Middle Triassic of Yunnan, China. *Acta Geologica Sinica - English Edition*

546 90:401–424. DOI: https://doi.org/10.1111/1755-6724.12680.

547

548 Cignoni P, Callieri M, Corsini M, Dellepiane M, Ganovelli F, Ranzuglia G. 2008. *MeshLab: an*

549 *Open-Source Mesh Processing Tool.* DOI:

550 10.2312/LocalChapterEvents/ItalChap/ItalianChapConf2008/129-136.

551

552 Close RA, Benson RBJ, Saupe EE, Clapham ME, Butler RJ. 2020. The spatial structure of

553 Phanerozoic marine animal diversity. *Science* 368:420–424. DOI: 10.1126/science.aay8309.

554

555 Dai X, Davies JHFL, Yuan Z, Brayard A, Ovtcharova M, Xu G, Liu X, Smith CPA, Schweitzer

556 CE, Li M, Perrot MG, Jiang S, Miao L, Cao Y, Yan J, Bai R, Wang F, Guo W, Song H,

557 Tian L, Dal Corso J, Liu Y, Chu D, Song H. 2023. A Mesozoic fossil lagerstätte from 250.8

558   million years ago shows a modern-type marine ecosystem. *Science* 379:567–572. DOI:

559   10.1126/science.adf1622.

560

561   Dick, DG, Maxwell EE. 2015. The evolution and extinction of the ichthyosaurs from the

562   perspective of quantitative ecospace modelling. *Biological Conservation* 11.

563

564   Fischer V, Bardet N, Benson RBJ, Arkhangelsky MS, Friedman M. 2016. Extinction of fish-

565   shaped marine reptiles associated with reduced evolutionary rates and global environmental

566   volatility. *Nature Communications* 7:10825. DOI: 10.1038/ncomms10825.

567

568   Fischer V, Bennion RF, Foffa D, MacLaren JA, McCurry MR, Melstrom KM, Bardet N. 2022.

569   Ecological signal in the size and shape of marine amniote teeth. *Proceedings of the Royal*

570   *Society B: Biological Sciences* 289:20221214. DOI: 10.1098/rspb.2022.1214.

571

572   Fischer V, Benson RBJ, Druckenmiller PS, Ketchum HF, Bardet N. 2018. The evolutionary

573   history of polycotylid plesiosaurians. *Royal Society Open Science* 5. DOI:

574   10.1098/rsos.172177.

575

576   Fischer V, Benson RBJ, Zverkov NG, Soul LC, Arkhangelsky MS, Lambert O, Stenshin IM,

577   Uspensky GN, Druckenmiller PS. 2017. Plasticity and convergence in the evolution of

578   short-necked plesiosaurs. *Current Biology* 27:1667–1676. DOI: 10.1016/j.cub.2017.04.052.

579

580   Fischer V, Maclaren JA, Bennion RF, Druckenmiller PS, Benson RBJ. 2020. The

581   macroevolutionary landscape of short-necked plesiosaurians. *Scientific Reports*.

582

583   Foffa D, Young MT, Stubbs TL, Dexter KG, Brusatte SL. 2018. The long-term ecology and

584   evolution of marine reptiles in a Jurassic seaway. *Nature Ecology & Evolution* 2:1548–

585   1555. DOI: 10.1038/s41559-018-0656-6.

586

587   Fröbisch NB, Fröbisch J, Sander PM, Schmitz L, Rieppel O. 2013. Macropredatory ichthyosaur

588   from the Middle Triassic and the origin of modern trophic networks. *Proceedings of the*

589   *National Academy of Sciences* 110:1393–1397. DOI: 10.1073/pnas.1216750110.

590

591   Furrer H. 1995. The Kalkschieferzone (Upper Meride Limestone, Ladinian) near Meride (Canton

592   Ticino, Southern Switzerland) and the evolution of a Middle Triassic intraplatform basin.

593   *Eclogae Geologicae Helvetiae* 88:827–852. DOI: 10.5169/seals-167706.

594

595   Furrer H. 2003. Der Monte San Giorgio im Südtessin - vom Berg der Saurier zur Fossil-

596   Lagerstätte internationaler Bedeutung.

597

598   Galili T. 2015. dendextend: an R package for visualizing, adjusting and comparing trees of

599   hierarchical clustering. *Bioinformatics* 31:3718–3720. DOI: 10.1093/bioinformatics/btv428.

600

601   Goloboff PA, Catalano SA. 2016. TNT version 1.5, including a full implementation of

602   phylogenetic morphometrics. *Cladistics*. DOI: 10.1111/cla.12160.

603

604 Griebeler EM, Klein N. 2019. Life-history strategies indicate live-bearing in *Nothosaurus*

605 (Sauropterygia). *Palaeontology* 62:697–713. DOI: https://doi.org/10.1111/pala.12425.

606

607 Guillerme T. 2018. dispRity: A modular R package for measuring disparity. *Methods in Ecology*

608 *and Evolution* In Press. DOI: 10.1111/2041-210X.13022.

609

610 Gutarra S, Rahman IA. 2022. The locomotion of extinct secondarily aquatic tetrapods. *Biological*

611 *Reviews* 97:67–98. DOI: https://doi.org/10.1111/brv.12790.

612

613 Heijne J, Klein N, Sander PM. 2019. The uniquely diverse taphonomy of the marine reptile

614 skeletons (Sauropterygia) from the Lower Muschelkalk (Anisian) of Winterswijk, The

615 Netherlands. *PalZ* 93:69–92. DOI: 10.1007/s12542-018-0438-0.

616

617 Hu S, Zhang Q, Chen Z-Q, Zhou C, Lü T, Xie T, Wen W, Huang J, Benton MJ. 2011. The

618 Luoping biota: exceptional preservation, and new evidence on the Triassic recovery from

619 end-Permian mass extinction. *Proceedings of the Royal Society B: Biological Sciences*

620 278:2274–2282. DOI: 10.1098/rspb.2010.2235.

621

622 Huang J, Motani R, Jiang D, Ren X, Tintori A, Rieppel O, Zhou M, Hu Y, Zhang R. 2020.

623 Repeated evolution of durophagy during ichthyosaur radiation after mass extinction

624 indicated by hidden dentition. *Scientific Reports* 10:7798. DOI: 10.1038/s41598-020-

625 64854-z.

626

627 Jiang D-Y, Lin W-B, Rieppel O, Motani R, Sun Z-Y. 2019. A new Anisian (Middle Triassic)

628   eosauropterygian (Reptilia, Sauropterygia) from Panxian, Guizhou Province, China. *Journal*

629   *of Vertebrate Paleontology* 38:1–9. DOI: 10.1080/02724634.2018.1480113.

630

631 Jiang D-Y, Motani R, Tintori A, Rieppel O, Chen G-B, Huang J-D, Zhang R, Sun Z-Y, Ji C.

632   2014. The Early Triassic eosauropterygian *Majiashanosaurus discocoracoidis*, gen. et sp.

633   nov. (Reptilia, Sauropterygia), from Chaohu, Anhui Province, People's Republic of China.

634   *Journal of Vertebrate Paleontology* 34:1044–1052. DOI: 10.1080/02724634.2014.846264.

635

636 Jiang D-Y, Schmitz L, Hao W-C, Sun Y-L. 2006. A New Mixosaurid Ichthyosaur from the

637   Middle Triassic of China. *Journal of Vertebrate Paleontology* 26:60–69.

638

639 Jiang D-Y, Schmitz L, Motani R, Hao W-C, Sun Y-L. 2007. The mixosaurid ichthyosaur

640   *Phalarodon* cf. *P. fraasi* from the Middle Triassic of Guizhou Province, China. *Journal of*

641   *Paleontology* 81:602–605. DOI: 10.1666/05092.1.

642

643 Kelley NP, Pyenson ND. 2015. Evolutionary innovation and ecology in marine tetrapods from

644   the Triassic to the Anthropocene. *Science* 348:aaa3716. DOI: 10.1126/science.aaa3716.

645

646 Klein N, Eggmaier S, Hagdorn H. 2022. The redescription of the holotype of *Nothosaurus*

647   *mirabilis* (Diapsida, Eosauropterygia)—a historical skeleton from the Muschelkalk (Middle

648   Triassic, Anisian) near Bayreuth (southern Germany). *PeerJ* 10:e13818. DOI:

649   10.7717/peerj.13818.

650

651 Klein N, Furrer H, Ehrbar I, Torres Ladeira M, Richter H, Scheyer TM. 2022. A new

652   pachypleurosaur from the Early Ladinian Prosanto Formation in the Eastern Alps of

653   Switzerland. *Swiss Journal of Palaeontology* 141:12. DOI: 10.1186/s13358-022-00254-2.

654

655 Klein N, Griebeler EM. 2016. Bone histology, microanatomy, and growth of the nothosauroid

656   *Simosaurus gaillardoti* (Sauropterygia) from the Upper Muschelkalk of southern

657   Germany/Baden-Württemberg. *Comptes Rendus Palevol* 15:142–162. DOI:

658   https://doi.org/10.1016/j.crpv.2015.02.009.

659

660 Klein N, Griebeler EM. 2018. Growth patterns, sexual dimorphism, and maturation modeled in

661   Pachypleurosauria from Middle Triassic of central Europe (Diapsida: Sauropterygia).

662   *Fossil Record* 21:137–157. DOI: 10.5194/fr-21-137-2018.

663

664 Klein N, Sander PM, Krahl A, Scheyer TM, Houssaye A. 2016. Diverse Aquatic Adaptations in

665   *Nothosaurus* spp. (Sauropterygia)—Inferences from Humeral Histology and Microanatomy.

666   *PLoS ONE* 11:e0158448.

667

668 Klein N, Voeten DFAE, Lankamp J, Bleeker R, Sichelschmidt OJ, Liebrand M, Nieweg DC,

669   Martin Sander P. 2015. Postcranial material of *Nothosaurus marchicus* from the Lower

670   Muschelkalk (Anisian) of Winterswijk, The Netherlands, with remarks on swimming styles

671   and taphonomy. *Paläontologische Zeitschrift* 89:961–981. DOI: 10.1007/s12542-015-0273-

672   5.

673

674   Klompmaker A, Fraaije R. 2011. The oldest (Middle Triassic, Anisian) lobsters from the

675   Netherlands: Taxonomy, taphonomy, paleoenvironment, and paleoecology. *Palaeontologia*

676   *Electronica* 14:1–15.

677

678   Krahl A. 2021. The locomotory apparatus and paraxial swimming in fossil and living marine

679   reptiles: comparing Nothosauroidea, Plesiosauria, and Chelonioidea. *PalZ* 95:483–501.

680   DOI: 10.1007/s12542-021-00563-w.

681

682   Krahl A, Klein N, Sander PM. 2013. Evolutionary implications of the divergent long bone

683   histologies of *Nothosaurus* and *Pistosaurus* (Sauropterygia, Triassic). *BMC Evolutionary*

684   *Biology* 13:1–23.

685

686   Li Q, Liu J. 2020. An Early Triassic sauropterygian and associated fauna from South China

687   provide insights into Triassic ecosystem health. *Communications Biology* 3:63. DOI:

688   10.1038/s42003-020-0778-7.

689

690   Lin W-B, Jiang D-Y, Rieppel O, Motani R, Tintori A, Sun Z-Y, Zhou M. 2021. *Panzhousaurus*

691   *Rotundirostris* Jiang et al., 2019 (Diapsida: Sauropterygia) and the Recovery of the

692   Monophyly of Pachypleurosauridae. *Journal of Vertebrate Paleontology*:e1901730. DOI:

693   10.1080/02724634.2021.1901730.

694

695   Lin K, Rieppel O. 1998. *Functional morphology and ontogeny of Keichousaurus hui (Reptilia,*

696   *Sauropterygia)*. Chicago Natural History Museum.

697

698   Liu J, Hu S, Rieppel O, Jiang D, Benton MJ, Kelley NP, Aitchison JC, Zhou C, Wen W, Huang

699   J, Xie T, Lv T. 2014. A gigantic nothosaur (Reptilia: Sauropterygia) from the Middle

700   Triassic of SW China and its implication for the Triassic biotic recovery. *Scient* 4:1–9. DOI:

701   10.1038/srep07142.

702

703   Liu J, Motani R, Jiang D-Y, Hu S-X, Aitchison JC, Rieppel O, Benton MJ, Zhang Q-Y, Zhou C-

704   Y. 2013. The first specimen of the Middle Triassic *Phalarodon atavus* (Ichthyosauria:

705   Mixosauridae) from South China, showing postcranial anatomy and peri-tethyan

706   distribution. *Palaeontology* 56:849–866.

707

708   Liu Q, Yang T, Cheng L, Benton MJ, Moon BC, Yan C, An Z, Tian L. 2021. An injured

709   pachypleurosaur (Diapsida: Sauropterygia) from the Middle Triassic Luoping Biota

710   indicating predation pressure in the Mesozoic. *Scientific Reports* 11:21818. DOI:

711   10.1038/s41598-021-01309-z.

712

713   Ma L, Jiang D, Rieppel O, Motani R, Tintori A. 2015. A new pistosauroid (Reptilia,

714   Sauropterygia) from the late Ladinian Xingyi marine reptile level , southwestern China.

715   *Journal of Vertebrate Paleontology* e881832:1–6. DOI: 10.1080/02724634.2014.881832.

716

717   MacLaren JA, Anderson PSL, Barrett PM, Rayfield EJ. 2017. Herbivorous dinosaur jaw

718   disparity and its relationship to extrinsic evolutionary drivers. *Paleobiology* 43:15–33. DOI:

719   DOI: 10.1017/pab.2016.31.

720

721   MacLaren JA, Bennion RF, Bardet N, Fischer V. 2022. Global ecomorphological restructuring

722   of dominant marine reptiles prior to the Cretaceous–Palaeogene mass extinction.

723   *Proceedings of the Royal Society B: Biological Sciences* 289:20220585. DOI:

724   10.1098/rspb.2022.0585.

725

726   Maisch MW, Matzke AT, Brinkmann W. 2006. The otic capsule of the Middle Triassic

727   ichthyosaur *Mixosaurus* from Monte San Giorgio (Switzerland): new evidence on the

728   braincase structure of basal ichthyosaurs. *Eclogae Geologiae Helvetiae* 99:205–210.

729

730   Maxwell EE, Diependaal H, Winkelhorst H, Goris G, Klein N. 2016. A new species of

731   *Saurichthys* (Actinopterygii: Saurichthyidae) from the Middle Triassic of Winterswijk, The

732   Netherlands. *Neues Jahrbuch für Geologie und Paläontologie - Abhandlungen* 280:119–

733   134. DOI: 10.1127/njgpa/2016/0569.

734

735   Maxwell EE, Romano C, Wu F, Furrer H. 2015. Two new species of *Saurichthys*

736   (Actinopterygii: Saurichthyidae) from the Middle Triassic of Monte San Giorgio,

737   Switzerland, with implications for character evolution in the genus. *Zoological Journal of*

738   *the Linnean Society* 173:887–912. DOI: 10.1111/zoj.12224.

739

740 de Miguel Chaves C, Ortega F, Pérez-García A. 2018. New highly pachyostotic nothosauroid

741   interpreted as a filter-feeding Triassic marine reptile. *Biology Letters* 14:20180130. DOI:

742   10.1098/rsbl.2018.0130.

743

744 Moon BC, Stubbs TL. 2020. Early high rates and disparity in the evolution of ichthyosaurs.

745   *Communications Biology* 3:68. DOI: 10.1038/s42003-020-0779-6.

746

747 Motani R. 1999. The skull and taxonomy of *Mixosaurus* (Ichthyopterygia). *Journal of*

748   *Paleontology* 73:924–935.

749

750 Motani R. 2009. The Evolution of Marine Reptiles. *Evolution: Education and Outreach* 2:224–

751   235. DOI: 10.1007/s12052-009-0139-y.

752

753 Motani R, Jiang D-Y, Tintori A, Sun Y-L, HaoWei-Cheng, Boyd A, Frlog-Hinic S, Schmitz L,

754   Shin J-Y, SunZuo-Yu. 2008. Horizons and assemblages of Middle Triassic marine reptiles

755   from Panxian, Guizhou, China. *Journal of Vertebrate Paleontology* 28:900–903.

756

757 Müller J. 2005. The anatomy of *Askeptosaurus italicus* from the Middle Triassic of Monte San

758   Giorgio and the interrelationships of thalattosaurs (Reptilia, Diapsida). *Canadian Journal of*

759   *Earth Sciences* 42:1347–1367. DOI: 10.1139/e05-030.

760

761 Neenan JM, Klein N, Scheyer TM. 2013. European origin of placodont marine reptiles and the

762   evolution of crushing dentition in Placodontia. *Nature Communications* 4:1621.

763

764   Neenan JM, Li C, Rieppel O, Scheyer TM. 2015. The cranial anatomy of Chinese placodonts and

765   the phylogeny of Placodontia (Diapsida: Sauropterygia). *Zoological Journal of the Linnean*

766   *Society*:In Press. DOI: 10.1111/zoj.12277.

767

768   Neenan JM, Reich T, Evers SW, Druckenmiller PS, Voeten DFAE, Choiniere JN, Barrett PM,

769   Pierce SE, Benson RBJ. 2017. Evolution of the Sauropterygian Labyrinth with Increasingly

770   Pelagic Lifestyles. *Current Biology*:1–7. DOI: 10.1016/j.cub.2017.10.069.

771

772   O'Keefe FR. 2002. The evolution of plesiosaur and pliosaur morphotypes in the Plesiosauria

773   (Reptilia: Sauropterygia). *Palaeobiology* 28:101–112.

774

775   Oksanen J, Blanchet FG, Friendly M, Kindt R, Legendre P, McGlinn D, Minchin RP, O'Hara

776   RB, Simpson GL, Solymos P, Stevens MHH, Szoecs E, Wagner H. 2019. vegan:

777   Community Ecology Package.

778

779   Paradis E, Claude J, Strimmer K. 2004. APE: Analyses of phylogenetics and evolution in R

780   language. *Bioinformatics* 20:289–290.

781

782   R Core Team. 2021. R: a language and environment for statistical computing.

783

784   Reeves JC, Moon BC, Benton MJ, Stubbs TL. 2021. Evolution of ecospace occupancy by

785   Mesozoic marine tetrapods. *Palaeontology* 64:31–49. DOI:

786   https://doi.org/10.1111/pala.12508.

787

788   Renesto S, Binelli G, Hagdorn H. 2014. A new pachypleurosaur from the Middle Triassic

789   Besano Formation of Northern Italy. *Neues Jahrbuch für Geologie und Paläontologie,*

790   *Abhandlungen* 271:151–168. DOI: 10.1127/0077-7749/2014/0382.

791

792   Revell LJ. 2012. phytools: An R package for phylogenetic comparative biology (and other

793   things). *Methods in Ecology and Evolution* E:217–223.

794

795   Rieppel O. 1992. A new species of the genus *Saurichthys* (Pisces: Actinopterygii) from the

796   Middle Triassic of Monte San Giorgio (Switzerland), with comments on the phylogenetic

797   interrelationships of the genus. *Palaeontographica Abteilung A* A221:63–94.

798

799   Rieppel O. 1994. *Osteology of Simosaurus gaillardoti and the relationships of stem-group*

800   *Sauropterygia.*

801

802   Rieppel O. 1999. Phylogeny and paleobiogeography of Triassic Sauropterygia: problems solved

803   and unresolved. *Palaeogeography, Palaeoclimatology, Palaeoecology* 153:1–15. DOI:

804   http://dx.doi.org/10.1016/S0031-0182(99)00067-X.

805

806 Rieppel O. 2000. *Sauropterygia I: Placodontia, Pachypleurosauria, Nothosauroidea,*

807   *Pistosauroidea*. F. Pfeil.

808

809 Rieppel O. 2002. Feeding mechanics in Triassic stem-group sauropterygians: the anatomy of a

810   successful invasion of Mesozoic seas. *Zoological Journal of the Linnean Society* 135:33–

811   63.

812

813 Rieppel O, Li C, Fraser NC. 2008. The skeletal anatomy of the Triassic protorosaur

814   *Dinocephalosaurus orientalis* Li, from the Middle Triassic of Guizhou Province, southern

815   China. *Journal of Vertebrate Paleontology* 28:95–110. DOI: 10.1671/0272-

816   4634(2008)28[95:TSAOTT]2.0.CO;2.

817

818 Rieppel O, Lin K. 1995. Pachypleurosaurs (Reptilia: Sauropterygia) from the Lower

819   Muschelkalk, and a review of the Pachypleurosauroidea. *Fieldiana Geology* 32:1–44.

820

821 Rieppel O, Wild R. 1996. A revision of the genus *Nothosaurus* (Reptilia: Sauropterygia) from

822   the Germanic Triassic, with comments on the status of *Conchiosaurus clavatus*. *Fieldana*

823   *(Geology)*.

824

825 Robin O'Keefe F, Otero RA, Soto-Acuña S, O'gorman JP, Godfrey SJ, Chatterjee S. 2017.

826   Cranial anatomy of *Morturneria seymourensis* from Antarctica, and the evolution of filter

827   feeding in plesiosaurs of the Austral Late Cretaceous. *Journal of Vertebrate Paleontology*

828   4634:e1347570. DOI: 10.1080/02724634.2017.1347570.

829

830 Röhl H-J, Schmid-Röhl A, Furrer H, Frimmel A, Oschmann W, Schwark L. 2001. Microfacies,

831   geochemistry and palaeoecology of the Middle Triassic Grenzbitumenzone from Monte San

832   Giorgio (Canton Ticino, Switzerland). *Geologia Insubrica* 6:1–13.

833

834 Sander PM. 1989. The pachypleurosaurids (Reptilia: Nothosauria) from the Middle Triassic of

835   Monte San Giorgio (Switzerland) with the description of a new species. *Philosophical*

836   *Transactions of the Royal Society of London. B, Biological Sciences* 325:561–666. DOI:

837   10.1098/rstb.1989.0103.

838

839 Sander PM, Griebeler EM, Klein N, Juarbe JV, Wintrich T, Revell LJ, Schmitz L. 2021. Early

840   giant reveals faster evolution of large body size in ichthyosaurs than in cetaceans. *Science*

841   374:eabf5787. DOI: 10.1126/science.abf5787.

842

843 Sander PM, Rieppel OC, Bucher H. 1997. A new pistosaurid (Reptilia: Sauropterygia) from the

844   Middle Triassic of Nevada and its implications for the origin of the plesiosaurs. *Journal of*

845   *Vertebrate Paleontology* 17:526–533. DOI: 10.1080/02724634.1997.10010999.

846

847 Sato T, Cheng Y-N, Wu X-C, Shan H-Y. 2014a. *Diandongosaurus acutidentatus* Shang, Wu &

848   Li, 2011 (Diapsida: Sauropterygia) and the relationships of Chinese eosauropterygians.

849   *Geological Magazine* 151:121–133. DOI: 10.1017/S0016756813000356.

850

851   Sato T, Zhao L-J, Wu X-C, Li C. 2014b. A new specimen of the Triassic pistosauroid

852   *Yunguisaurus*, with implications for the origin of Plesiosauria (Reptilia, Sauropterygia).

853   *Palaeontology* 57:55–76. DOI: 10.1111/pala.12048.

854

855   Scheyer TM, Neuman A, Brinkman D. 2019. A large marine eosauropterygian reptile with

856   affinities to nothosauroid diapsids from the Early Triassic of British Columbia, Canada.

857   *Acta Palaeontologica Polonica* 64. DOI: 10.4202/app.00599.2019.

858

859   Scheyer TM, Romano C, Jenks J, Bucher H. 2014. Early Triassic Marine Biotic Recovery: The

860   Predators' Perspective. *PLOS ONE* 9:e88987-.

861

862   Shang Q-H, Li C. 2015. A new small-sized eosauropterygian (Diapsida: Sauropterygia) from the

863   Middle Triassic of Luoping, Yunnan , southwestern China. *Vertebrata PalAsiatica* 53:265–

864   280.

865

866   Shang Q-H, Li C, Wang W. 2022. *Nothosaurus luopingensis* n. sp. (Sauropterygia) from the

867   Anisian, Middle Triassic of Luoping, Yunnan Province, China. DOI: 10.19615/j.cnki.2096-

868   9899.220524.

869

870   Shang Q-H, Wu X-C, Li C. 2020. A New Ladinian Nothosauroid (Sauropterygia) from Fuyuan,

871   Yunnan Province, China. *Journal of Vertebrate Paleontology* 40:e1789651. DOI:

872   10.1080/02724634.2020.1789651.

873

874   Spiekman SNF, Neenan JM, Fraser NC, Fernandez V, Rieppel O, Nosotti S, Scheyer TM. 2020.

875   Aquatic Habits and Niche Partitioning in the Extraordinarily Long-Necked Triassic Reptile

876   Tanystropheus. *Current Biology* 30:3889-3895.e2. DOI:

877   https://doi.org/10.1016/j.cub.2020.07.025.

878

879   Stayton CT. 2015. The definition, recognition, and interpretation of convergent evolution, and

880   two new measures for quantifying and assessing the significance of convergence. *Evolution*

881   69:2140–2153. DOI: 10.1111/evo.12729.

882

883   Stayton TristanC. 2018. convevol: Analysis of Convergent Evolution.

884

885   Stubbs TL, Benton MJ. 2016. Ecomorphological diversifications of Mesozoic marine reptiles:

886   the roles of ecological opportunity and extinction. *Paleobiology*:1–27. DOI:

887   10.1017/pab.2016.15.

888

889   Sutherland JTF, Moon BC, Stubbs TL, Benton MJ, Sutherland JTF. 2019. Does exceptional

890   preservation distort our view of disparity in the fossil record? DOI:

891   10.1098/rspb.2019.0091.

892

893   Suzuki R, Terada Y, Shimodaira H. 2019. pvclust: Hierarchical Clustering with P-Values via

894   Multiscale Bootstrap Resampling.

895

896 Thorne PM, Ruta M, Benton MJ. 2011. Resetting the evolution of marine reptiles at the Triassic-

897 Jurassic boundary. *PNAS* 108:8339–8344. DOI: 10.1073/pnas.1018959108.

898

899 Tschanz K. 1989. *Lariosaurus buzzii* n. sp. from the Middle Triassic of Monte San Giorgio

900 (Switzerland) with comments on the classification of nothosaurs. *Palaeontographica*

901 *Abteilung A* A208:153–179.

902

903 Vermeij GJ, Motani R. 2018. Land to sea transitions in vertebrates: the dynamics of colonization.

904 *Paleobiology* 44:237–250. DOI: 10.1017/pab.2017.37.

905

906 Wang W, Shang Q, Cheng L, Wu X-C, Li C. 2022. Ancestral body plan and adaptive radiation

907 of sauropterygian marine reptiles. *iScience* 25:105635. DOI:

908 https://doi.org/10.1016/j.isci.2022.105635.

909

910 Wu X-C, Cheng Y-N, Li C, Zhao L-J, Sato T. 2011. New information on *Wumengosaurus*

911 *delicatomandibularis* Jiang et al., 2008 (Diapsida: Sauropterygia), with a revision of the

912 osteology and phylogeny of the taxon. *Journal of Vertebrate Paleontology* 31:70–83. DOI:

913 10.1080/02724634.2011.546724.

914

915 Wu F, Sun Y, Fang G. 2017. A new species of *Saurichthys* from the Middle Triassic (Anisian) of

916 southwestern China. *VERTEBRATA PALASIATICA*. DOI: 10.19615/j.cnki.1000-

917 3118.071023.

918

919 Wu F, Sun Y, Hao W, Jiang D, Xu G, Sun Z, Tintori A. 2009. New species of *Saurichthys*

920 (Actinopterygii: Saurichthyidae) from Middle Triassic (Anisian) of Yunnan Province,

921 China. *Acta Geologica Sinica - English Edition* 83:440–450. DOI:

922 https://doi.org/10.1111/j.1755-6724.2009.00056.x.

923

924 Xu G-H, Ren Y, Zhao L-J, Liao J-L, Feng D-H. 2022. A long-tailed marine reptile from China

925 provides new insights into the Middle Triassic pachypleurosaur radiation. *Sicentific reports*

926 12. DOI: 10.1038/s41598-022-11309-2.

927

928 Xu G-H, Shang Q-H, Wang W, Ren Y, Lei H, Liao J, Zhao L, Li C. 2023. A new long-snouted

929 marine reptile from the Middle Triassic of China illuminates pachypleurosauroid evolution.

930 *Scientific Reports* 13:16. DOI: 10.1038/s41598-022-24930-y.

931

932 Zhang Q, Wen W, Hu S, Benton MJ, Zhou C, Xie T, Lü T, Huang J, Choo B, Chen Z-Q, Liu J,

933 Zhang Q. 2014. Nothosaur foraging tracks from the Middle Triassic of southwestern China.

934 *Nature communications* 5:1–12. DOI: 10.1038/ncomms4973.

935

936

Figure 1

Linear measurements used to calculate ecomorphological traits and example of Middle Triassic eosauropterygian craniodental architecture.

(A-H) linear measurements used to compute the ecomorphological traits used in our disparity analyses: (A,B) Cranial measurements shown on the 3D model of *Simosaurus gaillardoti* (SMNS 16363) in (A) dorsal and in (B) lateral views; (C) Tooth measurements shown on the 3D tooth model of *Simosaurus gaillardoti* (GPIT-PV-60638) in labial view; (D,E) mandibular measurements shown on the 3D model of *Nothosaurus giganteus* (SMNS 18058) in (D) dorsal and in (E) lateral views; (F) postcranial measurements (excepted on humerus and humerus) shown on the complete specimen of *Neusticosaurus edwardsii* (PIMUZ T2810); (G) humerus measurements shown on the 3D model of *Nothosaurus giganteus* (SMNS 81311); (H) femur measurements shown on the 3D model of *Nothosaurus giganteus* (SMNS 1589b). (I -L) examples of Middle Triassic eosauropterygian cranial architecture (I) *Anarodontus heterodontus* (NMNHL RGM443855); (J) *Nothosaurus mirabilis* (SMNS 13155); (K) *Simosaurus gaillardoti* (GPIT-PV-60638); (L) *Augustasaurus hagdorni* (FMNH PR1974). Colors indicate eosauropterygian clade; blue for Pachypleurosauroidea, orange for Nothosauroidea and purple for Pistosauroidea. Abbreviations: BCW, basal crown width; CH; crown height; DFFMT, distance fulcrum — first mandible tooth; DFMLT, distance fulcrum — last mandible tooth; DFMPAAM, distance fulcrum — mid-point of attachment of the adductor muscles; DL, dentigerous length; FL, femur proximodistal length; FW, femur width; FlL, forelimb length; FlW, forelimb width; HL, humerus proximodistal length; HW, humerus width; HlL, hindlimb length; HlW, hindlimb width; MH, mandible height; ML, mandible length; NeL; neck length; NL, naris length; OL, orbit length; OH, orbit height; OO, ocular offset; PL, parietal foramen length; RPL, retroarticular process length; PnL, prenarial length; SL, skull length; SW, skull width; SnL, snout length; SnW, snout width; SyL, symphysial length; TBL, total body length;

TaL, tail length; Trl, trunk length; UTFL, upper temporal fenestra length; UTFW, upper temporal fenestra width.
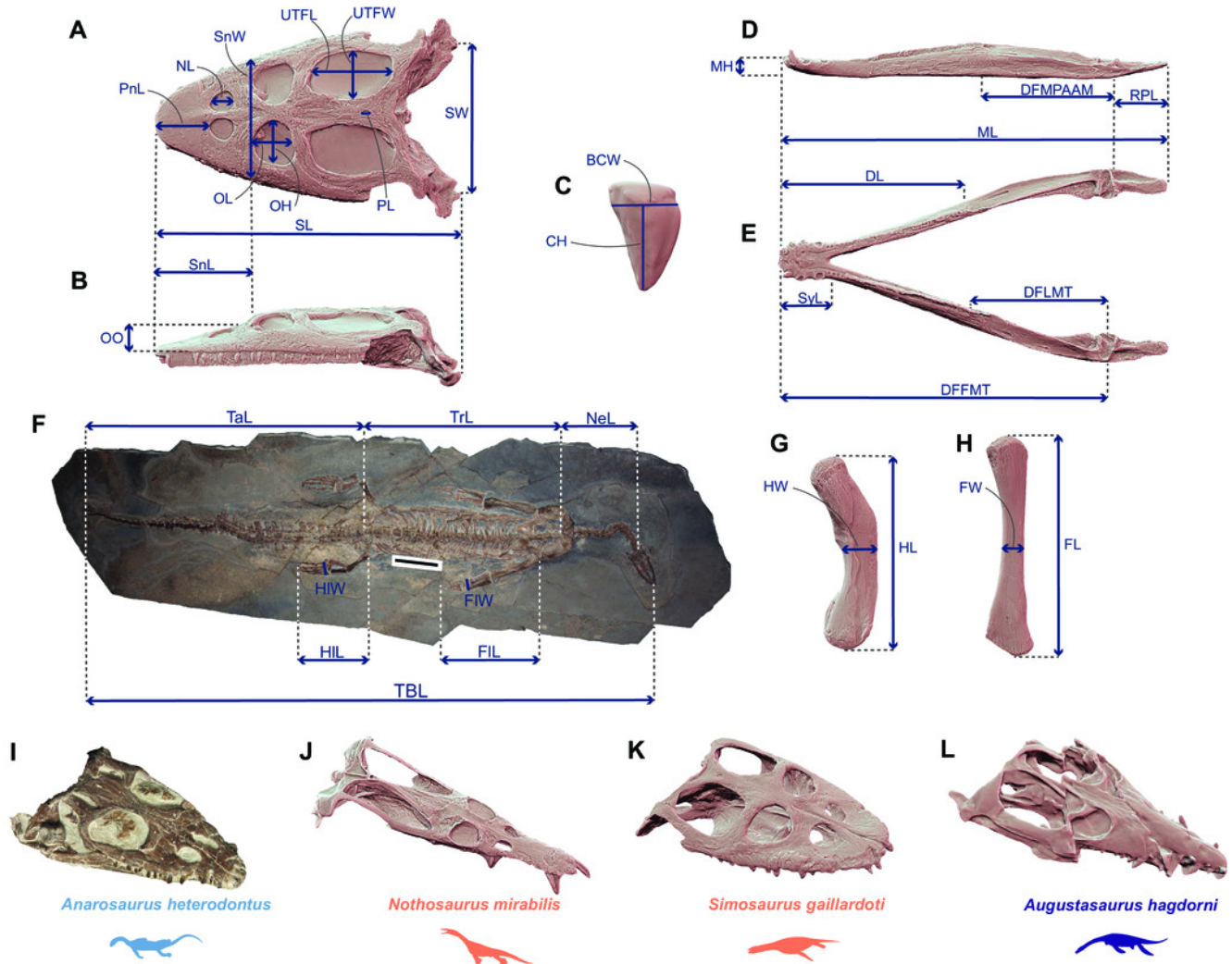
Figure 2

Functional ecomorphospace occupation, cluster dendrogram and size distribution in Middle Triassic eosauropterygians.

(A) Phylo-ecomorphospace occupation based on nonmetric multidimensional scaling (NMDS) axes (k=2) using the whole-body dataset, superimposed on the density of taxa. Data point sizes scaled to the relative skull size (log skull length). (B) Cluster dendrogram using the whole-body dataset. Values of the support of the main nodes (approximate unbiased p-value in percentage) have been indicated at their corresponding nodes. (C, D) Size distribution among pachypleurosauroids and nothosauroids: (C) log skull length, (D) log skull width.

A Macroevolutionary landscape

B Cluster dendrogram whole-body data

C Distribution of the skull length

D Distribution of the skull width

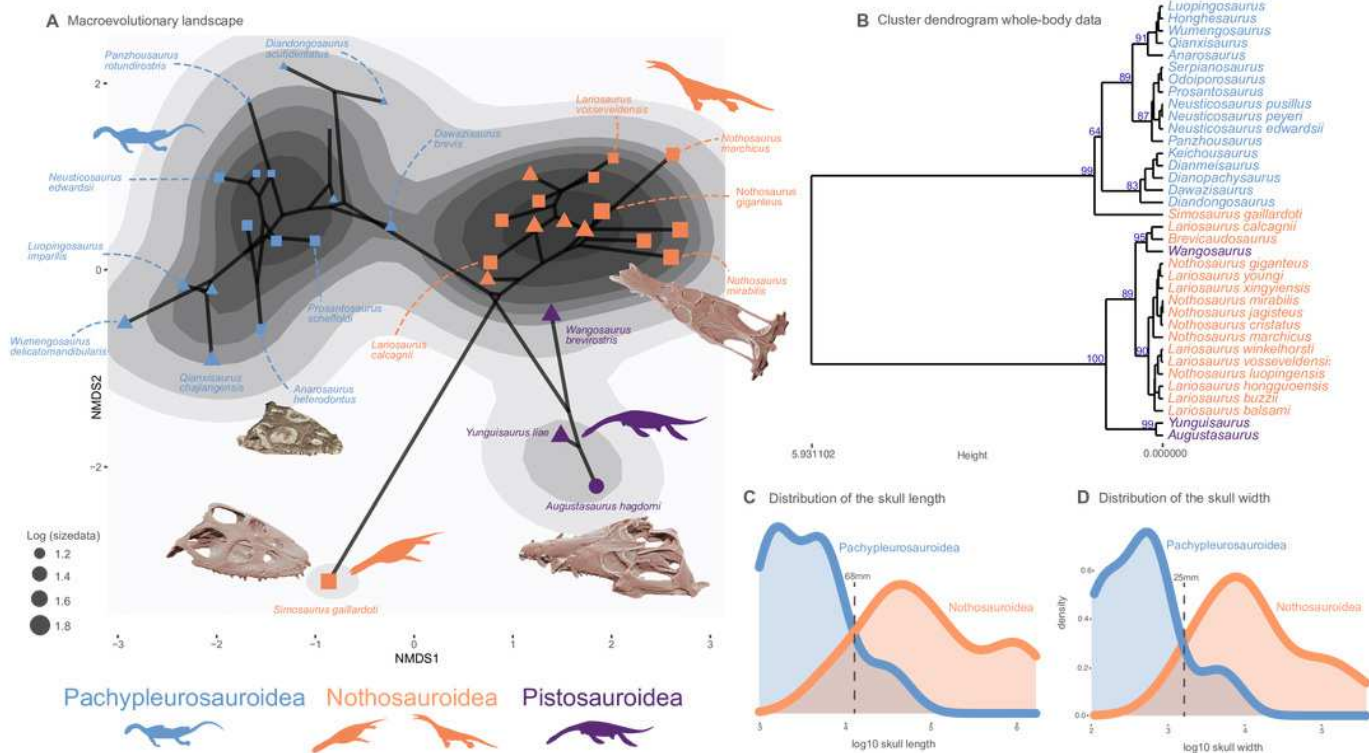Pachypleurosauroidea   Nothosauroidea   Pistosauroidea

Figure 3

Regional and temporal pachypleurosauroids and nothosauroids pattern of ecomorphological disparity.

(A) Paleobiogeography of the Middle Triassic, provided by Deep Time maps

https://deeptimemaps.com/map-room/ (Colorado Plateau Geosystem, 2016). (B and C)

comparison of the total disparity between the Western and Eastern Tethyan realm (B) for

pachypleurosauroids and (C) nothosauroids. (D-L) Evolution of eosauropterygian

ecomorphospace occupation during the Middle Triassic (D-I) in the Western Tethys and (J-L)

in the Eastern Tethys. Bithynian, Pelsonian and Illyrian are time bins of the Anisian while

Fassanian and Longobardian are time bins of the Ladinian. Eastern Tethys eosauropterygians

have only been found in the Pelsonian and Longobardian, in the Luoping, Panxian and Xingyi

biota respectively.

A

B Regional pachypleurosauroidean disparity 1000 boostraps

C Regional nothosauroidean disparity 1000 boostraps

D Western Tethys – all bins

E Bithynian

F Pelsonian

G Illyrian

H Fassanian

I Longobardian

J Eastern Tethys – all bins
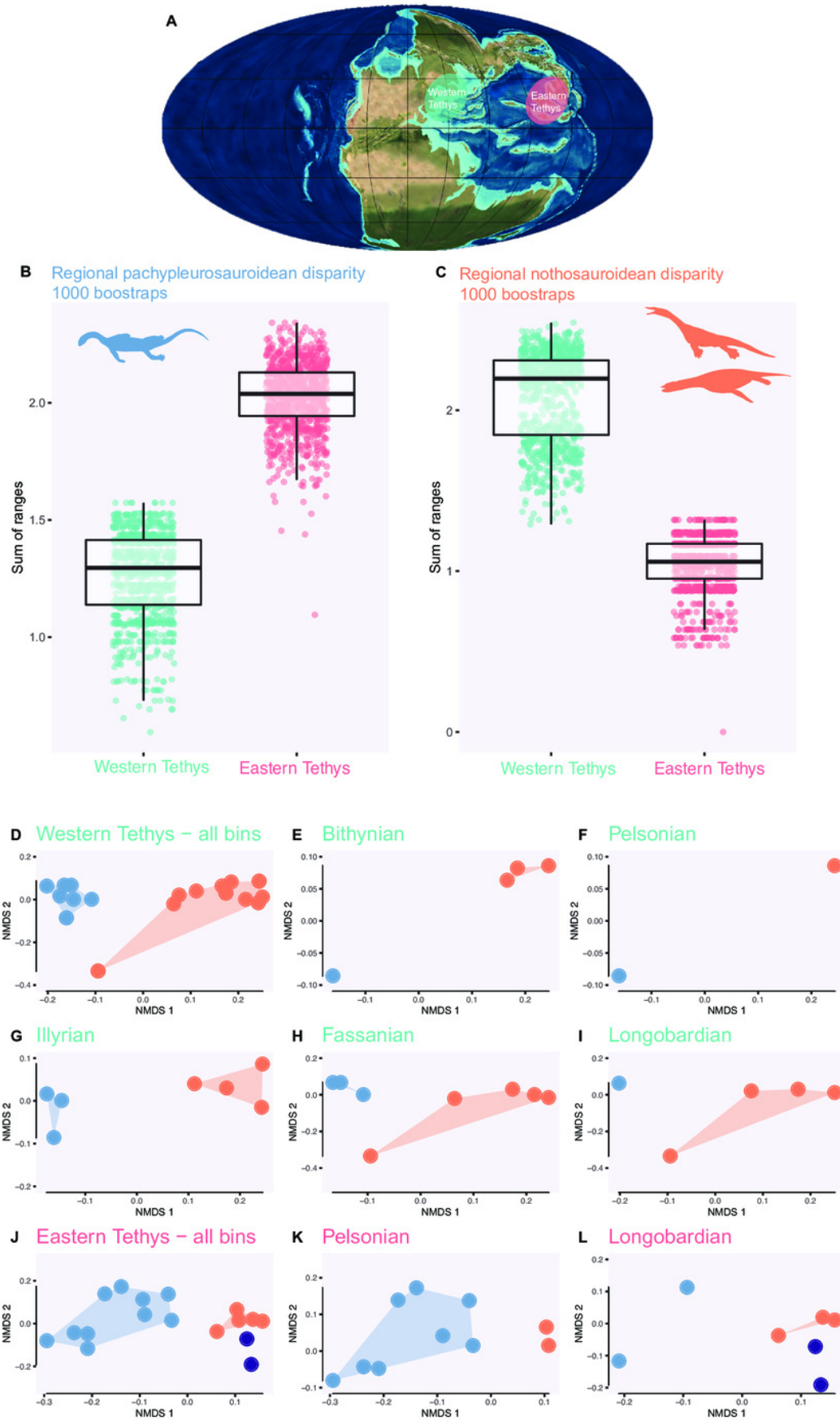
K Pelsonian

L Longobardian

Table 1(on next page)

List of specimens present in the analyses and data sources.

Taxon	Clade	Locality	Age range	Source of measurements
Anarosaurus heterodontus	Pachypleurosauroidea	Western Tethys	246.36 – 243.99	First-hand examination and photographs (Klein, 2009; 2012)
Dawazisaurus brevis	Pachypleurosauroidea	Eastern Tethys	244.94 – 243.99	Photographs (Cheng *et al.*, 2016)
Diandongosaurus acutidentatus	Pachypleurosauroidea	Eastern Tethys	244.94 – 243.99	Photographs (Shang *et al.*, 2011 and Sato *et al.*, 2013)
Dianmeiosaurus gracilis	Pachypleurosauroidea	Eastern Tethys	244.94 – 243.99	Photographs (Shang & Li, 2015)
Dianopachysaurus dingi	Pachypleurosauroidea	Eastern Tethys	244.94 – 243.99	Photographs (Liu *et al.*, 2011)
Honghesaurus longicaudalis	Pachypleurosauroidea	Eastern Tethys	244.94 – 243.99	Photographs (Xu *et al.*, 2022)
Luopingosaurus imparilis	Pachypleurosauroidea	Eastern Tethys	244.94 – 243.99	Photographs (Xu *et al.*, 2023)
Keichousaurus hui	Pachypleurosauroidea	Eastern Tethys	239.1 – 237	First-hand examination and photographs (Holmes & Cheng, 2008)
Neusticosaurus edwardsii	Pachypleurosauroidea	Western Tethys	239.1 – 237	First-hand examination
Neusticosaurus peyeri	Pachypleurosauroidea	Western Tethys	241.5 – 239.1	First-hand examination
Neusticosaurus pusillus	Pachypleurosauroidea	Western Tethys	241.5 – 239.1	First-hand examination
Odoiporosaurus teruzzi	Pachypleurosauroidea	Western Tethys	243.99 – 241.5	Photographs (Renesto *et al.*, 2014)
Panzhousaurus rotundirostris	Pachypleurosauroidea	Eastern Tethys	244.94 – 243.99	Photographs (Jiang *et al.*, 2019)
Prosantosaurus scheffoldi	Pachypleurosauroidea	Western Tethys	241.5 – 239.1	First-hand examination
Qianxisaurus chajiangensis	Pachypleurosauroidea	Eastern Tethys	239.1 – 237	Photographs (Cheng *et al.*, 2012)
Serpianosaurus mirigiolensis	Pachypleurosauroidea	Western Tethys	243.99 – 241.5	First-hand examination
Wumengosaurus delicatomandibularis	Pachypleurosauroidea	Eastern Tethys	244.94 – 243.99	Photogrpahs (Jiang *et al.*, 2008 and Wu *et al.*, 2020)
Brevicaudosaurus jiyangshanensis	Nothosauroidea	Eastern Tethys	239.1 – 237	Photographs (Shang *et al.*, 2020)
Lariosaurus calcagnii	Nothosauroidea	Western Tethys	241.5 – 239.1	First-hand examination
Lariosaurus balsami	Nothosauroidea	Western Tethys	239.1 – 237	First-hand examination
Lariosaurus buzzii	Nothosauroidea	Western Tethys	243.99 – 241.5	First-hand examination
Lariosaurus hongguoensis	Nothosauroidea	Eastern Tethys	244.94 – 243.99	Photographs (Jiang *et al.*, 2006)
Lariosaurus xingyensis	Nothosauroidea	Eastern Tethys	239.1 – 237	Photographs (Rieppel *et al.*, 2003 and Lin *et al.* 2017)
Lariosaurus vosseveldensis	Nothosauroidea	Western Tethys	246.36 – 243.99	Photographs (Klein *et al.*, 2016)
Lariosaurus winkelhorsti	Nothosauroidea	Western Tethys	246.36 – 244.94	First-hand examination, photographs made by the authors
Lariosaurus youngi	Nothosauroidea	Eastern Tethys	239.1 – 237	Photographs (Ji *et al.*, 2014)
Nothosaurus cristatus	Nothosauroidea	Western Tethys	239.1 – 237	First-hand examination
Nothosaurus luopingensis	Nothosauroidea	Eastern Tethys	244.94 – 243.99	Photographs (Shang *et al.*, 2022)
Nothosaurus giganteus	Nothosauroidea	Western Tethys	243.99 – 233.5	First-hand examination and 3D models created by the authors
Nothosaurus jagisteus	Nothosauroidea	Western Tethys	241.5 – 239.1	First-hand examination
Nothosaurus marchicus	Nothosauroidea	Western Tethys	246.5 – 241.5	First-hand examination, photographs (Klein *et al.*, 2015 and Voeten *et al.*, 2018)
Nothosaurus mirabilis	Nothosauroidea	Western Tethys	243.99 – 239.1	First-hand examination and 3D models created by the authors
Simosaurus gaillardoti	Nothosauroidea	Western Tethys	241.5 – 233.5	3D models created by the authors
Augustasaurus hagdorni	Pistosauroidea	Eastern Panthalassa	243.99 – 241.5	3D models created by the authors
Wangosaurus brevirostris	Pistosauroidea	Eastern Tethys	239.1 – 237	Photographs (Ma *et al.*, 2015)

| *Yunguisaurus liae* | Pistosauroidea | Eastern Tethys | 239.1 – 237 | Photographs (Cheng *et al.,* 2006 and Sato *et al.,* 2014) |

1
2

Table 2(on next page)

Table 2. List, definitions and completeness percentage of ecomorphological traits used in the disparity analyses.

The definition of each trait can be found in the Supplementary Information

Ecomorphological traits	Calculation	Percentage of completeness
Longirostry	Snout length / skull length	97.1
Snout shape ratio	Snout width / skull length	94.3
Jaw robusticity	Jaw height at mid-dentigerous length / mandible length	54.3
Relative symphysial length	Symphyseal length / mandible length	57.1
Functional toothrow	Dentigerous mandible length / mandible length	57.1
Anterior mechanical advantage	Distance between the fulcrum and the mid-point of attachment for the adductor muscles on the dorsal surface of the mandible / distance between the fulcrum and the anterior tip of mandible	68.6
Posterior mechanical advantage	Distance between the fulcrum and the mid-point of attachment for the adductor muscles on the dorsal surface of the mandible / distance between the fulcrum and the last mandibular tooth	54.3
Opening mechanical advantage	Distance between the fulcrum and the retroarticular process / distance between the fulcrum and the mid-point of attachment for the adductor muscles on the dorsal surface of the mandible	82.9
Nares position	Distance between the anterior margin of the nares and the tip of the snout / skull length	100
Relative naris size	Length of the nares / skull length	100
Relative orbit size	Mean diameter of the orbit / skull length	97.1
Occular offset	Distance from the centre of the orbit to the plane containing the upper tooth row / skull length	51.4
Relative parietal foramen length	Length of the parietal foramen / skull length	100
Tooth crown shape	Tooth crown height / crown base width	97.1
Absolute crown height	Tooth crown height raw measurement	100
Heterodonty index	Anterior tooth crown shape / posterior tooth crown shape	82.9
Jaw or snout anterior construction	Discrete character: (0) absence / (1) presence	94.3
Pointed and recurved tooth crowns	Discrete character: (0) absence / (1) presence	94.3
Bulbous crushing dentition	Discrete character: (0) absence / (1) presence	100
Enlarge procumbent dentition	Discrete character: (0) absence / (1) presence	100
Relative skull length	Skull length / trunk length	60
Relative neck length	Neck length / trunk length	60
Trunk proportion	Trunk length / body length	40
Tail proportion	Tail length / body length	40
Propodial variation	Humerus proximo-distal length / femur proximodistal length	77.1
Propodial size	Humerus proximo-distal length / skull length	77.1
Humerus gracility	Humerus antero-posterior width / humerus proximo-distal length	85.7
Femur gracility	Humerus antero-posterior width / humerus proximo-distal length	80
Forelimb aspect ratio	Forelimb antero-posterior width / forelimb proximo-distal length	51.4
Hindlimb aspect ratio	Hindlimb antero-posterior width / forelimb proximo-distal length	62.9

1

2

Table 3(on next page)

Results of the Stayton convergence tests for selected pairs of taxa using the first two and all the axes of PCoA analyses on the whole-body dataset and on the craniodental dataset for *S. gaillardoti* and *Q. chajiangensis.*

1
2

Taxon pair	PCo axes	C1	p-value	C2	p-value	C3	p-value	C4	p-value
Simosaurus gaillardoti – Qianxisaurus chajiangensis	PCo 1–2	0.2425	0.3197	0.0803	0.2537	0.1276	0.3506	0.0261	0.1888
	All axes	0.0000	0.9990	0.0000	0.9990	0.0000	0.9990	0.0000	0.9990
Wangosaurus brevirostris as a basal pistosauroidean – *Lariosaurus calcagnii*	PCo 1–2	0.7657	0.0220	0.1694	0.0270	0.4985	0.0000	0.1010	0.0090
	All axes	0.3174	0.0250	0.1042	0.0290	0.1637	0.0240	0.0320	0.0360
Wangosaurus brevirostris as a basal pistosauroidean– *Brevicaudosaurus jiyangshanensis*	PCo 1–2	0.8636	0.0080	0.2597	0.0000	0.5388	0.0000	0.1549	0.0000
	All axes	0.5452	0.0000	0.2520	0.0000	0.3576	0.0000	0.0773	0.0000
Wangosaurus brevirostris as a basal nothosauroidean– *Lariosaurus calcagnii*	PCo 1–2	0.7500	0.1555	0.0210	0.0210	0.3371	0.0220	0.1089	0.0100
	All axes	0.2166	0.0699	0.0620	0.0769	0.0889	0.1009	0.0225	0.1019
Wangosaurus brevirostris as a basal nothosauroidean – *Brevicaudosaurus jiyangshanensis*	PCo 1–2	0.7418	0.0210	0.1178	0.0480	0.5734	0.0000	0.0825	0.0360
	All axes	0.3385	0.0050	0.1076	0.0050	0.2290	0.0020	0.0391	0.0090

3